energies

MDPI

Review

Intelligent SOX Estimation for Automotive Battery Management Systems: State-of-the-Art Deep Learning Approaches, Open Issues, and Future Research Opportunities

Molla Shahadat Hossain Lipu [1,*], Tahia F. Karim [2], Shaheer Ansari [3], Md. Sazal Miah [4], Md. Siddikur Rahman [5], Sheikh T. Meraj [6], Rajvikram Madurai Elavarasan [7,*] and Raghavendra Rajan Vijayaraghavan [8]

1 Department of Electrical and Electronic Engineering, Green University of Bangladesh, Dhaka 1207, Bangladesh
2 Department of Electrical and Electronic Engineering, Primeasia University, Dhaka 1213, Bangladesh
3 Department of Electrical, Electronic and Systems Engineering, Universiti Kebangsaan Malaysia, Bangi 43600, Selangor, Malaysia
4 School of Engineering and Technology, Asian Institute of Technology, Pathum Thani 12120, Thailand
5 Department of Electrical and Electronics Engineering, Universiti Teknologi PETRONAS, Seri Iskandar 32610, Perak, Malaysia
6 Faculty of Science, Engineering and Built Environment, Deakin University, Geelong, VIC 3216, Australia
7 School of Information Technology and Electrical Engineering, The University of Queensland, St Lucia, QLD 4072, Australia
8 Automotive Department, Harman Connected Services India Pvt. Ltd., Bengaluru 560066, India
* Correspondence: shahadat@eee.green.edu.bd (M.S.H.L.); r.maduraielavarasan@uq.edu.au (R.M.E.)

Abstract: Real-time battery SOX estimation including the state of charge (SOC), state of energy (SOE), and state of health (SOH) is the crucial evaluation indicator to assess the performance of automotive battery management systems (BMSs). Recently, intelligent models in terms of deep learning (DL) have received massive attention in electric vehicle (EV) BMS applications due to their improved generalization performance and strong computation capability to work under different conditions. However, estimation of accurate and robust SOC, SOH, and SOE in real-time is challenging since they are internal battery parameters and depend on the battery's materials, chemical reactions, and aging as well as environmental temperature settings. Therefore, the goal of this review is to present a comprehensive explanation of various DL approaches for battery SOX estimation, highlighting features, configurations, datasets, battery chemistries, targets, results, and contributions. Various DL methods are critically discussed, outlining advantages, disadvantages, and research gaps. In addition, various open challenges, issues, and concerns are investigated to identify existing concerns, limitations, and challenges. Finally, future suggestions and guidelines are delivered toward accurate and robust SOX estimation for sustainable operation and management in EV operation.

Keywords: state of charge; state of health; state of energy; battery management system; electric vehicle; deep learning

Citation: Hossain Lipu, M.S.; Karim, T.F.; Ansari, S.; Miah, M.S.; Rahman, M.S.; Meraj, S.T.; Elavarasan, R.M.; Vijayaraghavan, R.R. Intelligent SOX Estimation for Automotive Battery Management Systems: State-of-the-Art Deep Learning Approaches, Open Issues, and Future Research Opportunities. *Energies* **2023**, *16*, 23. https://doi.org/10.3390/en16010023

Academic Editor: Abu-Siada Ahmed

Received: 2 December 2022
Revised: 15 December 2022
Accepted: 15 December 2022
Published: 20 December 2022

1. Introduction

Globally, emissions from transportation have been rising steadily, accounting for 27% of all emissions of carbon dioxide, 70% of which are produced by moving vehicles that burn fossil fuels [1]. The progress of electric vehicles (EV) has been a focal field of researchers and automotive engineers worldwide to solve these concerning difficulties [2,3]. Due to their advantages in terms of dependability, simplicity, comfort, and increased economy, EVs have emerged as the best replacement for diesel and petrol-powered cars [4,5]. They can also help reduce climate change, global warming, and environmental pollution-related issues. Due to the higher power density, lower self-discharge rate, high voltage, and long lifespan, lithium-ion batteries are currently commonly used in EVs [6,7]. The proper functioning of the battery storage system (BSS) depends on aging cycles, temperature rise, ongoing

electrochemical reactions, and material deterioration [8,9], which is crucial to ensure the efficient performance of EVs. In order to accurately measure temperature, current, and voltage in battery cells using proper switching, sensors, converters, controllers, thermal management system, and safety equipment, it is urgently necessary to develop an efficient and intelligent BMS [10–12].

Accurate and robust SOX estimation in terms of the state of health (SOH), state of energy (SOE), and state of charge (SOC) in EV BMS under uncertainties has grown to be urgent issues that demand significant attention [13–15]. SOC and SOE represent the state of charge and energy available in the battery, respectively, whereas SOH represents the battery's current health prognosis and remaining life [16]. The safe and dependable functioning of EVs is ensured by accurate prediction of SOX, which can prevent batteries from experiencing charging anomalies, overheating issues, and undesirable power breakdown occurrences [17,18]. However, SOX for BMSs is affected by a number of challenges, including slow convergence speed, complicated calculation, battery model design, algorithm development, and poor resilience due to temperature and noise changes [19,20]. Hence, the determination of an accurate and reliable SOX estimation for BMSs under various operating situations requires careful consideration and in-depth investigation.

Generally speaking, model-based techniques and machine learning (ML)-based strategies are used to estimate SOX in BMSs [21]. To effectively capture the behaviors of models, model-based approaches require a thorough grasp of their practical and theoretical backgrounds [22,23]. In accordance with this, model-based approaches use different complex computation equations and functional relationships relevant to the anodes, cathodes material features, and electrochemical processes, which often require extensive research and specialized knowledge to execute the experiments [24]. In contrast, ML-based algorithms examine SOX using a strong processor and big data set without any prior understanding of the complicated chemical interactions or the properties of battery materials [25,26]. The potential of traditional ML is greatly expanded by high-configuration computer processors, advanced graphics processing units (GPU), and expanding the number of computational layers due to the rise in data size [27]. Deep learning (DL) methods, the upgraded form of machine learning, have drawn a lot of interest in SOC, SOH, and state of power (SOP) estimates because of their enhanced learning ability, improved generalization efficiency, and higher precision [28,29]. The effectiveness of DL approaches, however, is dependent on the availability of a significant quantity of data as well as suitable hyperparameter combinations and choice of structure [30]. As a result, more research is required to develop reliable SOC, SOH, and SOP algorithms that have a sufficiently low computational cost.

The most promising technique for processing, managing, and monitoring massive data is now known to be deep learning (DL). The scientific community has been drawn to DL because of recent developments in different sectors, comprising healthcare [31], image processing [32], and voice recognition [33]. Even so, no research has been carried out on reviews based on DL in SOX estimation for intelligent BMSs. Noteworthy review articles that have recently been published concentrated on ML-based techniques and model-based approaches for robust SOC, SOH, and SOE estimations for BMSs. For instance, a survey by Xiong et al. examined the performance of SOH [13] and SOC [34] for BMSs based on various model-based approaches, emphasizing the techniques, advantages, disadvantages, and potential developments. Shrivastava et al. [35] employed the Kalman filter technique for real-time SOC estimation whereas another classification-based SOH estimation topology for lithium-ion batteries was described by Tian et al. [36]. SOC estimation utilizing numerous data-driven techniques was investigated by Dickson et al. [37]. Li et al. [38] performed an analysis of SOH prediction in both ML and analytical modeling techniques. Lipu et al. concentrated on major concerns, obstacles, and potential for data-driven SOC [39] and SOH [40] estimation approaches. SOC was examined by Hannan et al. [41] for investigating advantages, drawbacks, accuracy, and difficulties. The prediction of SOH for lithium-ion batteries was provided by Yang et al. [42]. A work by Zhang et al. [43] covered the hybrid approach, the adaptive filter method, and the SOC learning approach. Berecibar et al. [44]

adopted experimental and adaptive approaches for estimating SOH for lithium-ion BMSs. The various techniques for SOH and SOC estimation in EV batteries utilizing ML techniques were discussed by Vidal et al. [45]. Concurrently, a comparative analysis of the various works discussed earlier has been tabulated in Table 1, depicting the area of research and the research gap. The aforementioned research demonstrates major improvements in SOX estimation toward achieving better performance, utilizing either ML approaches or model-based techniques. Nonetheless, a review study concentrating on DL techniques for SOX estimation has not received much attention.

Table 1. Focused area and research gaps of the existing literature.

Reference	Focused Area	Research Gap
[37]	Delivered a review of the various data-driven techniques for SOC estimation	Review based on other state estimations, such as SOH and SOP, was not conducted
[39]	Reviewed data-driven techniques for SOC estimation	DL technique-based review for SOC estimation was not performed
[40]	SOH and RUL estimation techniques were investigated	The review was not comprehensive
[42]	Focused on a review of SOH estimation techniques	DL technique for SOH and other state estimation was not carried out
[45]	Studied various machine learning techniques for SOC estimation	The implementation factor for SOC estimation was not reviewed

This study presents new contributions by providing a thorough analysis of SOX estimation for BMSs utilizing DL approaches in order to address the previously mentioned research gaps. This paper's originality comes in its evaluation of DL concerning state-of-the-art approaches, key findings, problems, concerns, and potential future aspects for SOC, SOE, and SOH estimation. This review includes these cutting-edge contributions:

- State-of-the-art DL approaches for SOX estimation concerning SOC, SOE, and SOH are comprehensively reviewed. In line with that, the structure, strengths, shortcomings, verification profiles, factors, and estimate errors of various DL-enabled SOX estimations are thoroughly examined.
- The main concerns and issues of DL techniques are discussed in relation to battery components, operations, and algorithms.
- Fruitful recommendations and future research opportunities for DL-based SOX estimation for smart BMSs are provided.

There are six sections in this paper. Section 1 outlines the background, rationale, and research gaps of recent studies and the contributions of the proposed review article. Section 2 narrates the survey framework for article inclusion/exclusion criteria. Section 3 explains the preliminaries of various DL approaches applied in BMSs. Section 4 highlights various DL algorithms for SOX estimation. Section 5 explores the problems and difficulties in estimating battery SOX. Finally, this study concludes with various suggestions and improvements in Section 6.

2. Survey Methodology

The conducted review article aims to develop an important and crucial assessment of various SOX estimation techniques based on DL techniques for automotive BMSs. This review was conducted by observing various steps based on screening and analysis which were divided into three phases to select relevant articles, as presented in Figure 1. The first phase of the screening process was based on the analysis of various web platforms, such as IEEE Xplore, ScienceDirect, MDPI, Google Scholar, etc., to select suitable articles for this review. The second phase was conducted by applying various keywords used for battery SOX estimation, such as SOC, SOH, SOE, lithium-ion batteries, battery management systems, and electric vehicles. Furthermore, the selection was based on the title, abstract,

novelty, contributions, and research gaps. The final screening was conducted based on criteria such as the journal's quartile, citation, impact factor, and review process. In this way, a total of 101 articles were selected for conducting this review of DL technique-based SOX estimation for automotive applications.

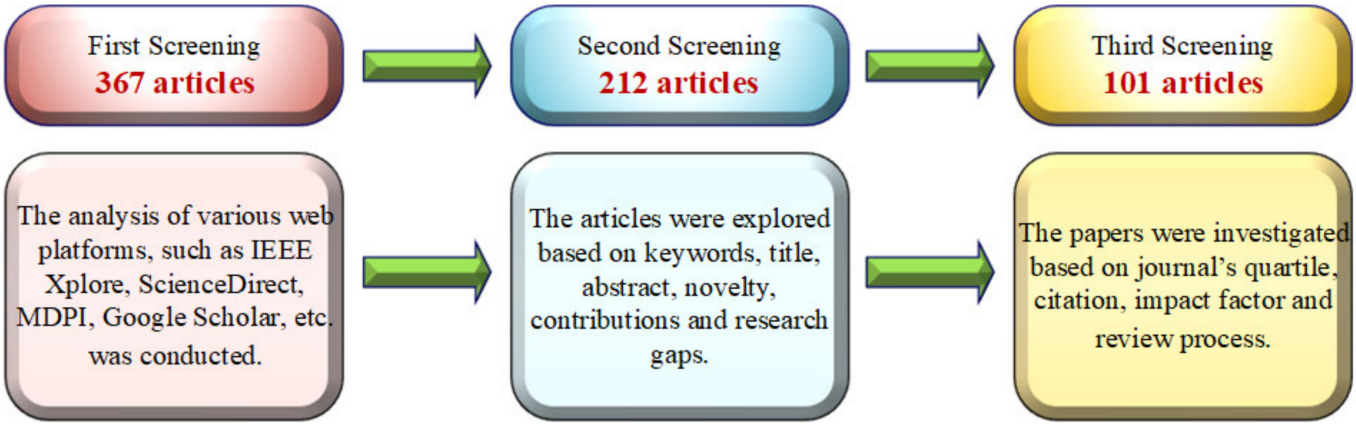

Figure 1. The survey framework for appropriate article selection criteria.

The outcomes of the screening and analysis were classified into four categories. At first, state-of-the-art DL methods, operations, and execution processes for SOX estimation were discussed. Secondly, the assessment of various DL technique-based SOX estimation methods was reviewed in detail. Thirdly, critical issues and concerns for the implementation of DL in SOX estimation were discussed. Fourthly, the conclusion was presented with prospects and suggestions.

3. State-of-the-Art Deep Learning Algorithms Applied in Intelligent Battery Management Systems

Recently, the application of DL models consisting of several layers with sophisticated structures has been applied in automotive research for model development, training, and analysis with a large volume of data [46]. DL models execute operations with activation functions and training algorithms using multiple hidden layers and neurons compared to the single hidden layer in a simple neural network model [47]. Commonly employed DL models in SOX estimation are LSTM, GRU, CNN, and autoencoder models. The configuration, computational implementation equations, advantages, and disadvantages of various DL models are presented in Table 2.

The execution of DL approaches for SOX estimation can be allocated into three phases. The first phase includes appropriate battery selection, data collection, data extraction, data preprocessing, and data division into training and testing, as depicted in Figure 2.

The second phase covers a DL network structure that depends on lots of factors, including suitable hyperparameter selection, such as hidden layers, hidden neurons, learning rate, decay rate, weight, bias initialization, number of iterations, batch size, and number of epochs, as denoted in Figure 3. Moreover, the accuracy of DL-based SOX estimation is subject to selecting appropriate training and testing functions and operations, including backpropagation, gradient descent, activation functions (Sigmoid, tanh, and ReLU), an Adam optimizer, and ensemble optimization.

Table 2. Structure, mathematical expressions, advantages, and disadvantages of DL approaches.

Method	Structure	Mathematical Expressions	Advantages	Disadvantages
LSTM	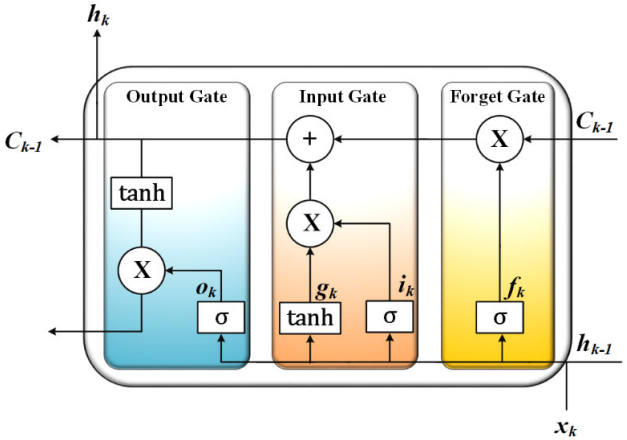	$f_k = \sigma\left(W_f\ [h_{t-1},\ x_k] + b_f\right)$ $i_k = \sigma\left(W_i\ [h_{t-1},\ x_k] + b_i\right)$ $g_k = tanh\left(W_c\ [h_{t-1},\ x_k] + b_c\right)$ $C_t = f_k * C_{t-1} + i_k * g_k$ $o_k = \sigma\left(W_o\ [h_{t-1},\ x_k] + b_o\right)$ $h_t = o_k * tanh\left(C_t\right)$	Requires no fine adjustment; regulates better flow of information through each gate.	Long training time; needs more memory for model training.
GRU	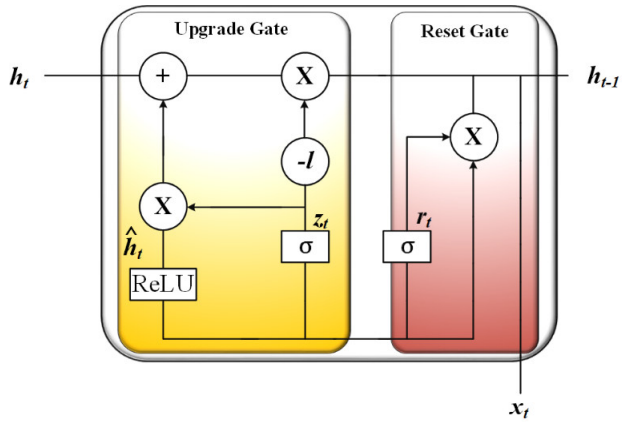	$z_t = \sigma\left(W_z\ [h_{t-1},\ x_k]\right)$ $r_t = \sigma\left(W_r\ [h_{t-1},\ x_k] + b_o\right)$ $\hat{h}_k = tanh\left(W_o\ [r_t *\ \ h_{t-1},\ x_k]\right)$ $h_t = (1 - z_t) * h_{t-1} + z_t * h_t$	Requires less memory and demonstrates fast training speed; removes vanishing gradient issues.	Slow convergence rate and low learning efficiency.

Table 2. *Cont.*

Method	Structure	Mathematical Expressions	Advantages	Disadvantages
CNN	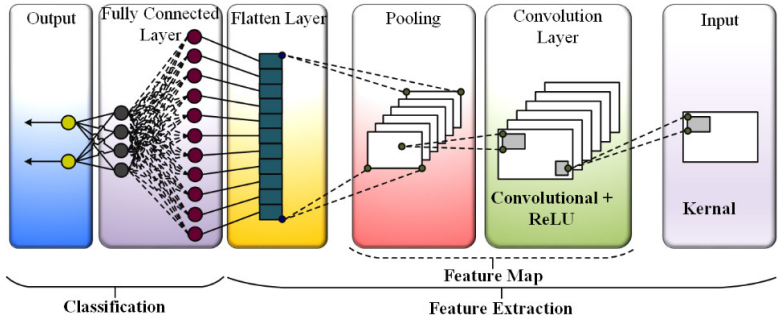	$\frac{A+2B-C}{D+1}$ $y_i^{(l)} = B_i^{(l)} + \sum_{j=1}^{m_1^{(l-1)}} k_{i,j}^{(l)} * y_j^{(l-1)}$ $y_i^{(l)} = f z_i^{(l)}$ $z_i^{(l)} = \sum_{j=1}^{m_1^{(l-1)}} \sum_{r=1}^{m_2^{(l-1)}} \sum_{s=1}^{m_3^{(l-1)}} w_{i,j,r,s}^{(l)} (Y_j^{(l-1)})_{r,s}$	Ability to detect important features without human intervention.	Lacks capabilities to trace the position and orientation of the object.
Autoencoder	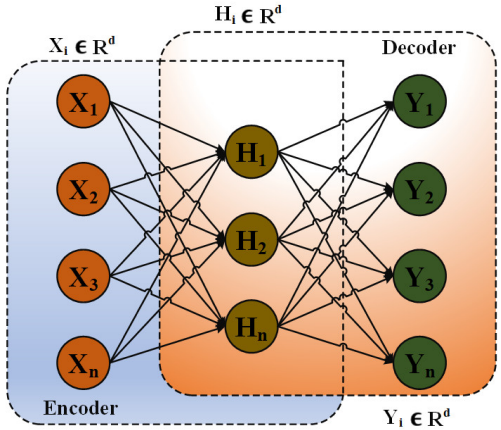	$h_m = f' x_m$ $x'_m = g' h_m$	Better feature extraction ability; efficient training due to noise-reducing capability in input data.	Requires more data for effective training, more computational time, and hyperparameter adjustments.

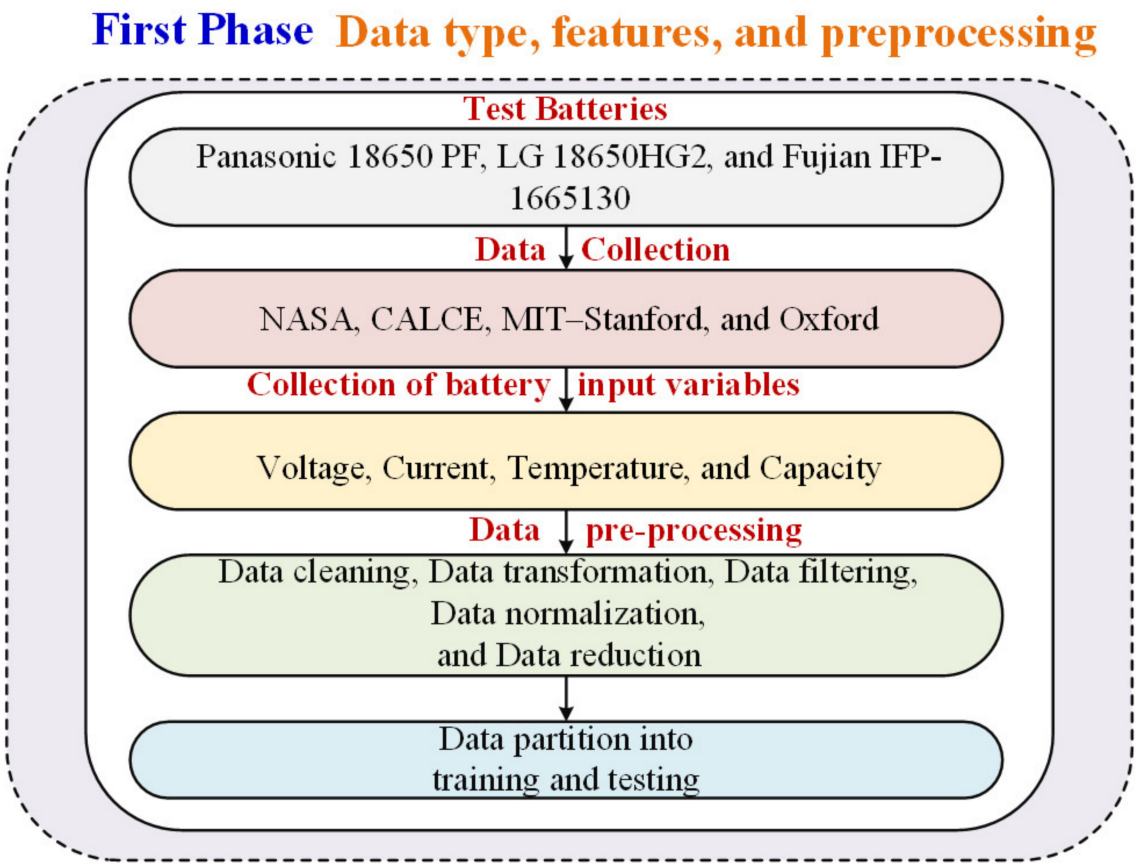

Figure 2. Data preparation and preprocessing for SOX estimation in automotive BMS.

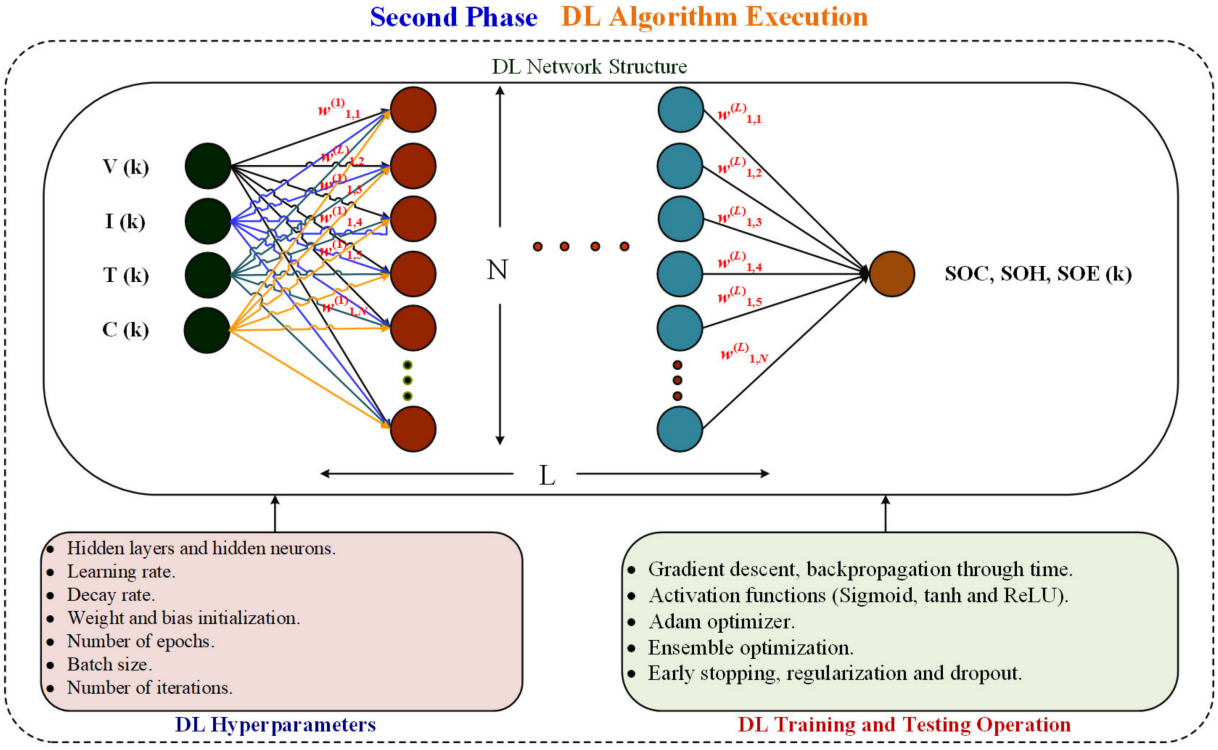

Figure 3. DL algorithm structure, execution, hyperparameters, and operation.

The third phase consists of the validation and verification of DL methods using various statistical error terms and performance assessments under a fixed ambient temperature

and varying ambient temperatures. Moreover, the performance is further verified under noise and aging impacts. In addition, a comparative analysis with the recent literature can be carried out to check a DL-based SOX estimation in terms of accuracy and robustness. Furthermore, hardware-in-the-loop tests and prototype hardware validation can still be conducted. Performance validation procedures are shown in Figure 4.

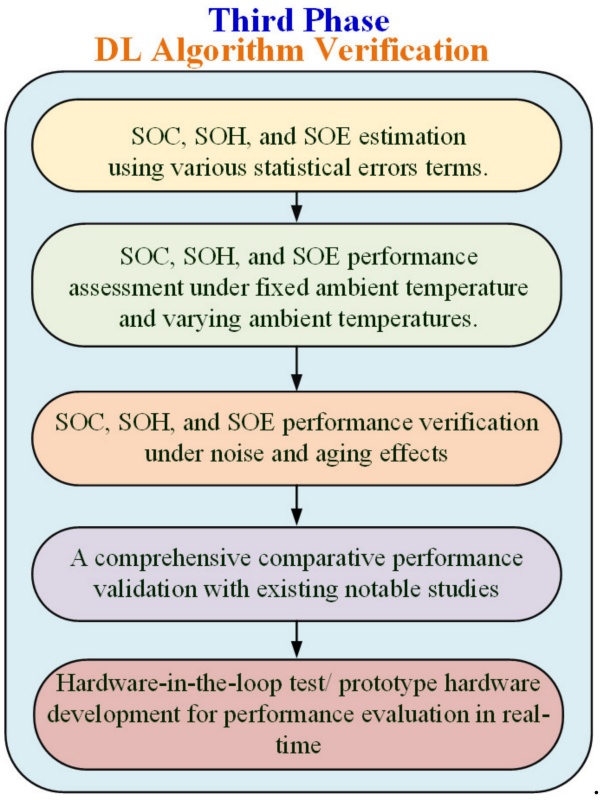

Figure 4. The performance validation procedures for DL-based SOX estimation.

4. Deep Learning-Enabled SOX Estimation Frameworks

This section delivers an overview of various DL models and frameworks implemented in SOX estimation in automotive BMS applications. This critical discussion focuses on various important aspects, including targets, contributions, key findings, DL structure, battery types, thermal condition, valuation process, results, and research gaps.

4.1. LSTM Framework for SOX Estimation

The LSTM model is one of the most effective DL techniques employed for the SOX estimation of lithium-ion batteries. The LSTM model is usually employed due to its ability to eliminate the vanishing gradient problem and to increase model training accuracy for SOX estimation.

4.1.1. LSTM-Based SOC Estimation Approaches

Chen et al. [48] developed a SOC estimation framework with an LSTM model considering the extended inputs and constrained output. The experimentations were performed on a battery dataset attained from the Center for Advanced Life Cycle Engineering (CALCE) and based on loading conditions similar to the Federal Urban Driving Schedule (FUDS) and Dynamic Stress Testing (DST). The validation of the proposed model was conducted based on different temperatures, such as 0 °C, 10 °C, 20 °C, 30 °C, 40 °C, and 50 °C, respectively. The LSTM model was also validated with different intelligent models, and the results concluded that the SOC error of the proposed LSTM model was lower contrasted with other NN approaches. Although the validation was conducted based on different operating

temperatures, further assessment can still be conducted based on different battery datasets. Almaita et al. [49] proposed an LSTM algorithm-based SOC estimation of high-capacity grid-scale lithium-ion BSSs so that the power profile in the power system could be improved. The battery dataset was attained from AL-Manara PV power in Jordan which consisted of a battery storage capacity of 12 MWh. Three important battery features, temperature, current, and voltage, were considered for the SOC estimation. The LSTM model was validated with a feedforward neural network (FFNN) and deep feedforward neural network (DFFNN). The outcomes depicted that the LSTM model was highly accurate with a mean squared error (MSE) of 0.62% compared to the SOC of the DFFNN and FFNN in the ranges of 4.03% to 7.37% and 5.37% to 9.22%, respectively. The LSTM-based SOC estimation delivered satisfactory outcomes and can be implemented in high-capacity BSSs. Nonetheless, the justification of the suggested approach with another battery dataset can be used in further research activities. Oyewola et al. [50] improvised the LSTM approach to develop a controllable deep transfer learning (CDTL) network for SOC estimation, as presented in Figure 5. The suggested CDTL network enhanced the target LSTM for long-term SOC estimation. The MIT Stanford battery database consisting of 124 lithium-ion battery datasets was employed for the proposed work. However, only three battery datasets were chosen for the experimentation. The CDTL network achieved higher SOC estimation accuracy with a root means square error (RMSE) of 0.70% compared to the benchmark approaches, such as LSTM and autoencoder. The proposed CDTL model enhanced transfer learning capability by 50%; however, the algorithm demonstrated high complexity for hardware implementation.

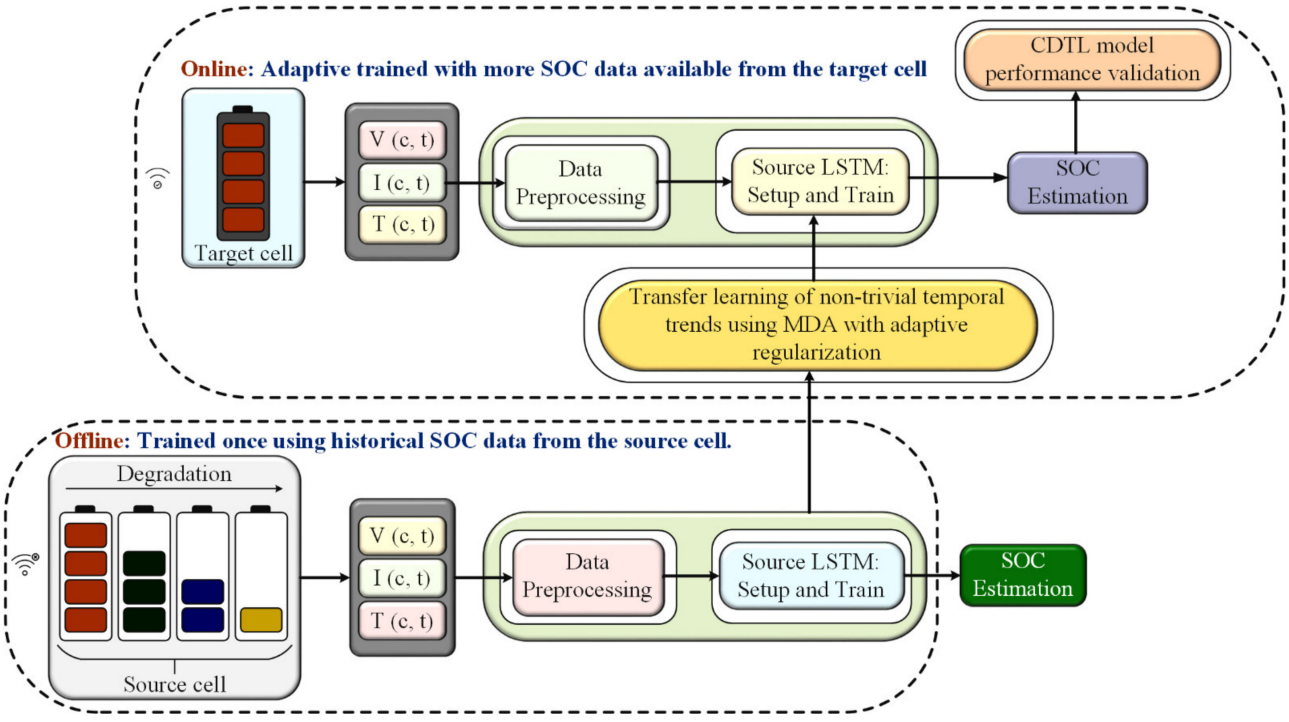

Figure 5. Improved LSTM model-based SOC estimation framework.

A hybrid LSTM and extended Kalman filter approach with wide temperature adaptation for SOC estimation was developed by Aninnakwa et al. [51]. The SOC estimation with LSTM and EKF model was conducted under cold (−10 °C), normal (25 °C), and hot (50 °C) temperatures. The experiment was conducted on an LNCM70Ah (lithium nickel manganese cobalt oxide) lithium-ion battery under varying operating temperatures. The results for the SOC estimation under the HPPC condition denoted the best mean absolute error (MAE), root means square error (RMSE), and R^2 values of 0.0697%, 0.0784%, and 99.9965%, respectively, while the RMSE, MAE, and R^2 values estimated were 0.0779%, 0.0943%, and

99.9842% under DST conditions. The proposed model delivered results with the inclusion of more training time compared with the conventional LSTM model, which can be reduced by considering other aging factors and working conditions. A particle swarm optimized (PSO) LSTM model was developed for the SOC estimation of lithium-ion batteries [52]. The PSO model was employed to optimize the fundamental factors of the LSTM model to match the data features with the network structure. The experimentation was conducted on li-ion batteries with a nominal voltage of 3.2 V and nominal capacity of 6.2 Ah. The verification of the PSO-LSTM model was carried out with models such as EKF and conventional LSTM. A PSO-optimized LSTM model was introduced for SOC estimation by Ren et al. [52]. The PSO technique was employed to explore the suitable key parameters of the LSTM model. The batteries used in the experiments were LiFePO4 batteries with a nominal capacity and nominal voltage of 6.2 Ah and 3.2 V, respectively. The appropriate use of noisy data was added for assessing the robustness of the LSTM-PSO approach.

4.1.2. LSTM-Based SOH Estimation Approaches

Ma et al. [53] developed an improved LSTM model and considered various health indicators, such as discharge capacity, temperature, current, and voltage, to develop a data framework for the model training. The Pearson correlation coefficient was applied to select the appropriate health indicators with a high correlation with the output capacity. Additionally, a differential evolution grey wolf optimizer (DEGWO) was used to select the optimal hyperparameters of the LSTM model. Two battery datasets, namely NASA and MIT Stanford battery datasets, were employed for the testing and validation. It was depicted that the SOH estimation error was within 1% for both battery datasets. This method depicts high potential for practical application; nonetheless, this model depicts high complexity due to the execution of the DL model with an optimization technique, and hence a suitable hyperparameter selection technique may be employed. Gong et al. [54] proposed a PSO technique-based LSTM model for SOH estimation of li-ion batteries. The execution of PSO was conducted for a better selection of model hyperparameters. The experiment was conducted on 18650-26 J lithium-ion batteries with a nominal capacity of 2.6 Ah. The validation of the PSO-LSTM model was compared to other models, such as a back propagation neural network (BPNN), support vector regression (SVR), and conventional LSTM model. For the proposed model, the RMSE (%) was within 1% compared with other models. However, further validation of the PSO-LSTM model can still be conducted with other metaheuristic optimization techniques. A SOH estimation technique with Bayesian optimization (BO) and an LSTM model was introduced by He et al. [55]. The battery experimental tests were conducted on the real data of EV applications concerning user behavior. The SOH estimation accuracy was measured based on RMSE and MAE where the BO-LSTM model delivered an RMSE of 7.552% and MAE of 1.521%. Real-time EV data was employed for the SOH estimation of lithium-ion batteries; nevertheless, the proposed model can be validated with other models to depict its accuracy and effectiveness. Li et al. [56] suggested an RUL and SOH estimation scheme based on a variant long short-term memory (VLSTM) model. The model used four health indicators, temperature, current, voltage, and time, for SOH estimation. The experiments were performed on 28 battery datasets acquired from the NASA battery database. The results demonstrated the high effectiveness and accuracy of the proposed model with an RMSE of 0.0159. Cui et al. [57] developed an integrated LSTM and UKF-based SOH estimation framework for lithium-ion batteries. The application of UKF with the LSTM model was observed to eliminate unwanted noises and reduce estimation errors. The datasets were acquired from the NASA Ames Prognostics Center of Excellence, consisting of four battery datasets, namely B33, B36, B41, and B42, respectively. It was observed that the proposed LSTM-UKF models performed satisfactorily compared to the reference model [58]. The work lacks comprehensive validation results; however, further work can still be conducted toward the development of a coestimation framework for SOC and SOH based on the same model features. A conventional LSTM model for SOH estimation was proposed by Wu et al. [59]. The voltage parameters from

the charging and discharging profile along with the incremental capacity profile were analyzed, and suitable features relating to the capacity degradation curve were extracted. The experiment was carried out by considering five batteries based on two types with different sizes and nominal capacities. The algorithm execution was conducted utilizing the different percentages of the training dataset, such as 30%, 40%, 50%, 60%, and 70%. The model validation was based on different data-driven model outcomes in terms of performance error indicators, such as MAE, mean squad error (MSE), RMSE, and R^2.

4.1.3. LSTM-Based SOE Estimation Approaches

Fan et al. [60] developed a hybrid LSTM-AUKF model-based coestimation framework for SOC and SOE, as shown in Figure 6. The battery dataset was acquired from the CALCE battery database. The LSTM-UKF model was validated with various dynamic driving schedules under different initial errors and operating temperatures. The performance error based on RMSE and MAE delivered appropriate outcomes of 0.46% and 0.44%, respectively. Additionally, the LSTM-AUKF model was computationally more effective compared to other models, such as autoencoder-LSTM models and forgetting factor-based adaptive EKF algorithms. Further research can still be conducted based on embedded BMS test platforms and validation in real-time applications.

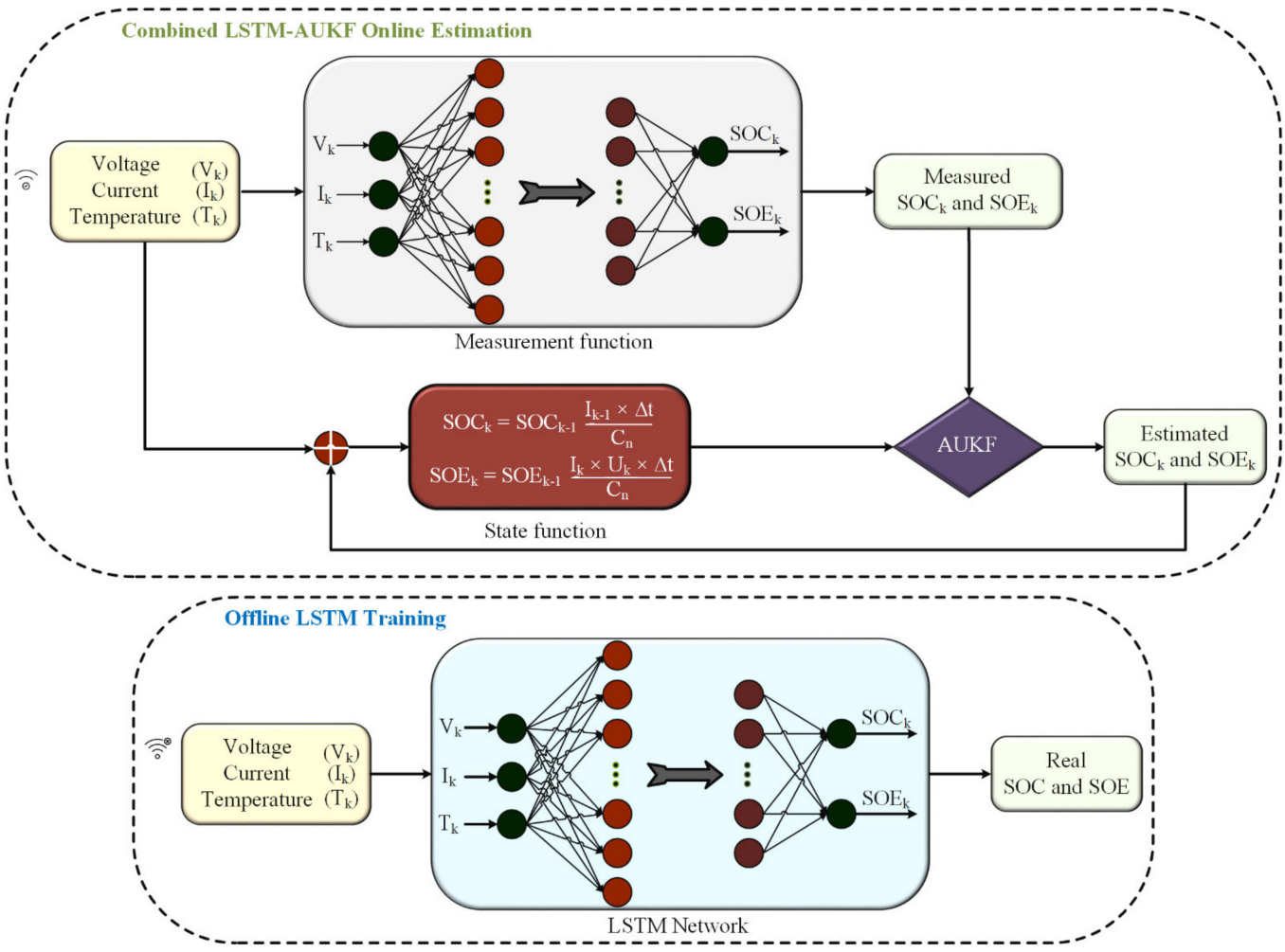

Figure 6. LSTM-AUKF model-based co-estimation of SOE and SOC.

An LSTM-based model for SOC and SOE estimation of li-ion batteries was presented by Ma et al. [61]. The battery dataset was acquired from the public datasets provided by Dr. Phillip Kollmeyer. The experiment was conducted on a single Panasonic 18650PF battery

cell with a nominal voltage of 3.6 V and nominal capacity of 2.9 Ah. The dataset includes battery charging and discharging values at different current ratings, EV, and mixed drive cycles under different temperature settings. The validation was performed based on two dynamic drive cycles under noise interference, different battery materials, and different initial temperatures. The achieved MAE for the SOE was 1.09% under fixed temperature, 0.64% for different battery materials, and 1.19% for noise features. High accuracy and robustness with SOE estimation were achieved; however, a suitable selection of the model hyperparameters can be performed carefully. The summary of LSTM-based SOX estimation is highlighted in Table 3.

4.2. GRU Framework for SOX Estimation

GRU models have been suitably adopted in SOX estimations for lithium-ion batteries. GRU models eliminate the issue of vanishing gradient problems and, furthermore, require less memory space for model training.

4.2.1. GRU-Based SOC Estimation Approaches

Wang et al. [62] developed an enhanced GRU model based on transfer learning for SOC estimation with battery datasets extracted from CALCE, UW–Madison, and NASA employed with nominal capacities of 2000 mAh, 2900 mAh, and 2000 mAh and a nominal voltage of 3.6 V. Three battery parameters, namely voltage, current and temperature, were extracted to prepare the dataset for executing model training. The validation of the improved GRU model was performed with the LSTM model, which delivered the SOC estimation outcomes with a training time of 441.15 s whereas the proposed GRU model delivered the SOC estimation outcomes within 387.37 s. However, further research may be accomplished with more sophisticated DL models and metaheuristic optimization techniques. Chen et al. [63] suggested a SOC estimation of lithium-ion batteries by developing a hybrid GRU and AKF model, as depicted in Figure 7. The hybrid GRU-AKF model limited the inaccuracies during the current fluctuations and delivered accurate SOC estimation. The conducted work employed battery datasets obtained from CALCE at the University of Maryland under different driving conditions. It is observed that the RMSE and maximum error (MAXE) were less than 1.3% and 2.2%, respectively. The hybrid GRU-AKF demonstrated satisfactory SOC outcomes with an improved efficiency and convergence speed of less than 1 s.

Cui et al. [64] developed an improved bidirectional GRU (BGRU) and YKF based on real-time SOC estimation techniques at different operating temperatures. Two driving cycles, namely the Urban Dynamometer Driving Schedule (UDDS) and US06, were employed to validate the proposed method. A satisfactory SOC estimation accuracy was achieved at different operating conditions; the RMSE and ME were less than 1.12% and 0.83%, respectively. However, further work can be undertaken to develop a hybrid method consisting of a neural network and KF technique. A GRU-RNN-based SOC estimation technique was framed by Jiao et al. [65]. Two battery parameters, namely voltage and current, were utilized to develop an appropriate data framework for model training. A momentum term was introduced to optimize the weights of the network and accelerate the SOC convergence speed. The battery data extraction was conducted from the battery testing setup named NEWARE CT-4008-5V12A comprising batteries with a nominal capacity of 2.2 Ah. The outcomes of the SOH estimation with a momentum gradient were evaluated based on different noise variances, different epochs, and different hidden neurons. It was suggested that the proposed approach can be applied to the RUL estimation of the supercapacitor.

Table 3. Summary of LSTM-based SOX estimation approaches.

SOX Estimation	Structure	Battery Chemistry	Thermal Status	Validation Process	Results	Research Gaps
SOC [49]	-Number of hidden neurons 22 -Learning rate 0.01 -Number of epochs 150	Not mentioned	Room temperature	With another neural network, such as DFFNN and FFNN	-MSE 0.62% (model 1) -MSE 0.60% (model 2) -MSE 0.48% (model 3)	Appropriate selection of model hyperparameters and deeper validation with other DL models, such as CNN and GRU
SOC [50]	-Number of hidden neurons 10 -Number of epochs 20 -Batch size 64	Lithium iron phosphate/graphite (LFP) cells	30 °C	With conventional LSTM model	-RMSE 0.70% -MAE 0.48%	Application of transfer learning for nonparametric Bayesian model for SOC estimation can be conducted
SOC [51]	-Number of hidden neurons 30 -Learning rate 0.01 -Number of epochs 300	LNCM battery	−10 °C, 25 °C, and 50 °C	With conventional LSTM model, different temperatures, and HPPC working condition	MAE = 0.0697%, RMSE = 0.0784%, R^2 = 99.9965%	Consideration of different battery chemistries for the validation can be performed
SOH [54]	For PSO: -Population size 5 -Number of iterations 50 -C1 1.5 -C2 1.5	18,650 size lithium-ion batteries	Room temperature	With another neural network such as BPNN, LSTM, and SVR	For A1: -RMSE 1.7572% -MAE 2.3350%	Depicts complexity due to the application of optimization technique with DL model
SOH [55]	-Number of hidden layers 2 -Number of epochs 400 -Dropout coefficient 0.5	Not mentioned	0–10 °C, 10–20 °C, 20–30 °C, 30–40 °C, and greater than 40 °C.	-No validation was conducted based on other models and temperatures	-RMSE 7.552% -MAE 1.521%	The validation with other models was not conducted
SOH [59]	Not mentioned	18,650 size lithium-ion batteries	Room temperature	With another neural network, such as ELM, SVM, and GPR model	For cell 3 -MAE 4.67% -MSE 1.66 × 10^{-4} -RMSE 1.29%	Appropriate use of optimization technique can be employed for suitable selection of model hyperparameters
SOE [61]	-Number of layers 3 -Number of neurons 256, 8, 2 -Number of epochs 100 -Learning rate 0.001	Panasonic 18650PF cell	Data collection was conducted at 0 °C, 10 °C, and 25 °C	With different drive cycles and temperatures	RMSE at 10 °C and 25 °C for UDDS drive cycle 2.88%, 1.61%	Other state estimation techniques can be integrated into future research

4.2.2. GRU-Based SOH Estimation Approaches

Chen et al. [66] developed a GRU approach-based SOH estimation technique for lithium-ion batteries, as displayed in Figure 8. Apart from the GRU model, the ELM method was used to forecast the entire temperature variation, and KF was employed to smoothen the data. The experimentation was performed by extracting eight commercial kokam pouch cell suitable battery datasets from the University of Oxford. The hyperparameter of the GRU model was selected by the trial and error (TE) technique by changing the number of hidden neurons. The RMSE, mean absolute error (MAE), and MAXE were within the limits of 1.2%, 1.02%, and 2.28%, respectively. In future research, more emphasis can be given to the extraction of more varying and extensive datasets based on different operating temperatures for model training.

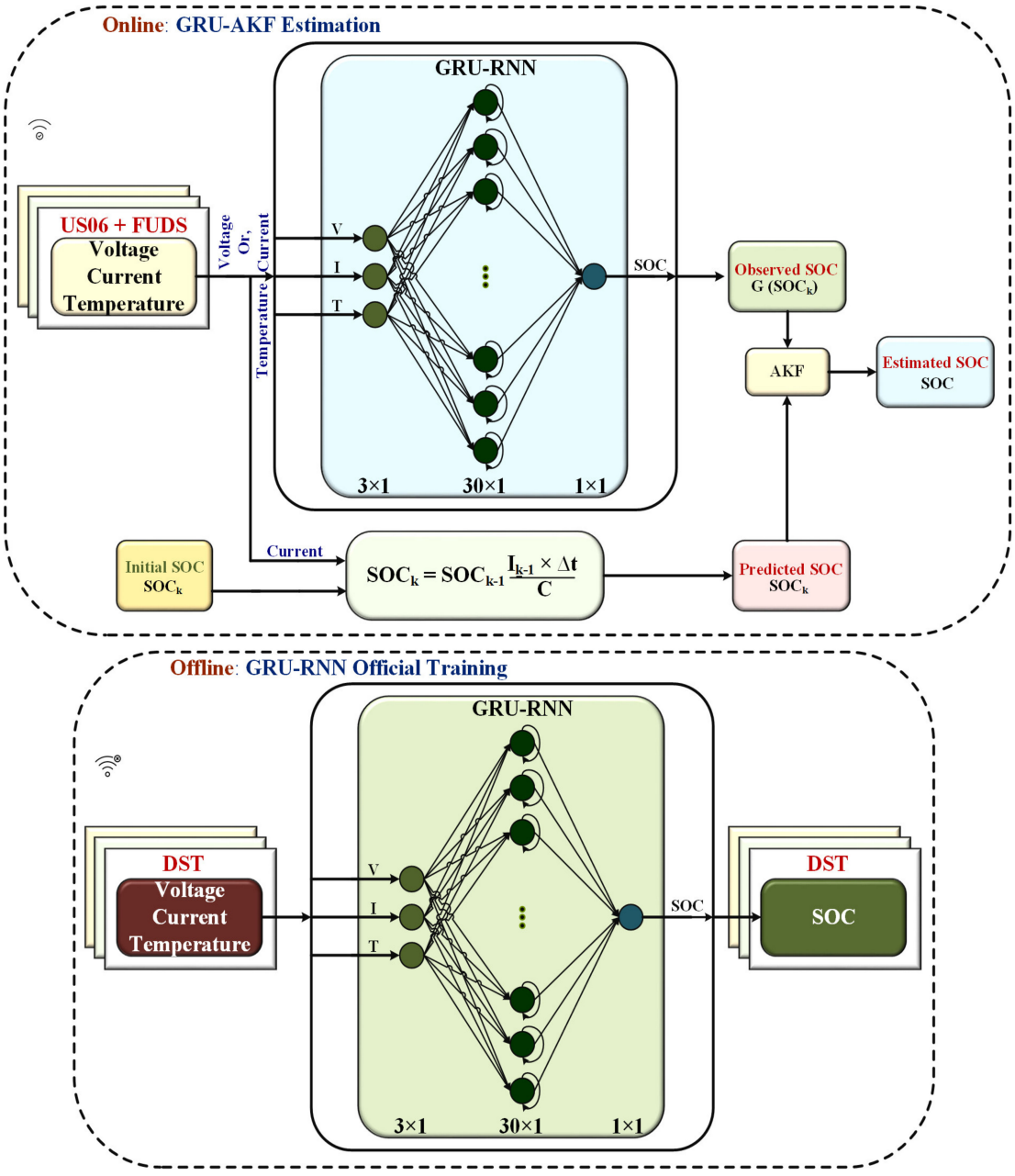

Figure 7. Hybrid GRU-AKF model-based SOC estimation framework.

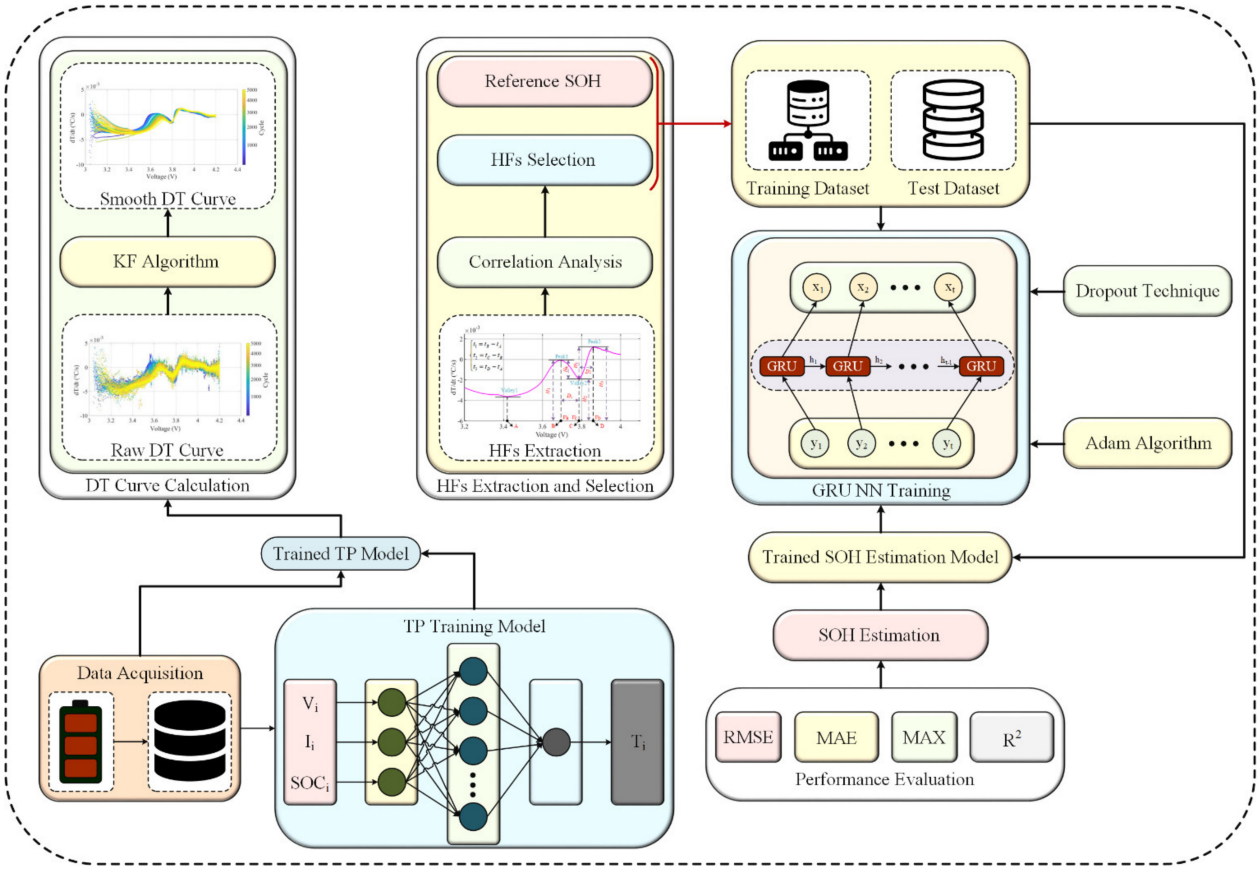

Figure 8. GRU model-based SOH estimation framework for BMS.

Fan et al. [67] developed a hybrid GRU and CNN model for SOH estimation of lithium-ion batteries. The proposed GRU-CNN-based hybrid model can work under the time dependencies of a charging curve. Two online battery datasets were employed from NASA and Oxford to conduct the experiments. Four battery datasets, namely RW 16, RW 20, RW 24, and RW 28, were acquired from the NASA database whereas cell 4 and cell 8 were acquired from the Oxford battery database. The GRU-CNN model surpassed other models, such as SVR, GPR, CNN, and the conventional GRU-based model on SOH estimation accuracy by delivering a MAXE of 4.11% and 1.62% for the NASA battery dataset and Oxford battery dataset, respectively. However, the proposed model demonstrated high computational complexity with a training time of 60,193.27 s compared to 57,268.44 s for GRU, 4237.71 s for CNN, 446.71 s for GPR, and 10,316.18 s for the SVR model. Cui and Joe [68] developed a spatial–temporal attention-based GRU model for the prediction of lithium-ion BMSs. The proposed work extracted six health indicators from battery charging and discharging profiles that could correlate with the battery aging process. Model training and testing were carried out on the three NASA battery datasets, i.e., B0005, B0006, and B0007, respectively. The proposed model delivered satisfactory SOH estimation outcomes based on minimum MAE and RMSE and outperformed other models, such as SVM, GPR, RNN, LSTM, and conventional GRU. Fan et al. [67] introduced a GRU-CNN-based hybrid SOH estimation scheme for lithium-ion BMSs considering time dependencies of the battery charging profile. Three battery parameters, namely voltage, current, and temperature, were used for constructing the data framework for model training. The battery dataset was extracted from the NASA battery database consisting of 28 battery datasets divided into seven groups. The verification and assessment of the GRU-CNN model was performed with different data-driven models, such as SVR, GPR, CNN, and GRU model, respectively. The GRU-CNN model depicted superiority based on the lowest SOH error; however, the model complexity depicted issues related to high training time, which could be improved

in further research. The contributions of GRU-based SOX estimation under different conditions are presented in Table 4.

Table 4. Summary of GRU-based SOX estimation approaches.

SOX Estimation	Structure	Battery Chemistry	Thermal Status	Validation Process	Results	Research Gaps
SOC [63]	-Number of hidden neurons 30 -Number of epochs 300 -Learning rate 0.01 -Batch size 64	$LifePO_4$ battery	The battery dataset was gathered from 8 different temperature profiles, i.e., −10 °C, 0 °C, 10 °C, 20 °C, 25 °C, 30 °C, 40 °C, and 50 °C	With other driving cycle datasets and other data-driven models	for US06 -RMSE 1.1% -MAXE 2.2% -Computational time 0.0862 s	Validation with other battery chemistries was not conducted.
SOC [64]	-Number of epochs 1000 -Number of hidden neurons 300	18,650 size li-ion batteries	−20 °C, −10 °C, and 0 °C	The validation was conducted with different temperatures	At 0 °C (UDDS) -MAE 0.0221 -RMSE 0.0311 -R^2 0.9880	Validation and improvement in SOC estimation over varying temperature ranges.
SOC [65]	-Number of epochs 400 -Number of hidden neurons 30	BTcap 21,700 lithium battery	Max/min charging temperature 20 °C/55 °C	The validation process was based on different model hyperparameters	Momentum gradient: For hidden neurons as 30 -RMSE 0.0152 -MAE 0.0100 -R^2 0.9972	The framework did not represent a complete framework and lacked critical points associated with methodology and results.
SOH [66]	-Number of hidden layers 2 -Number of hidden neurons 60 -Batch size 32 -Dropout rate 0.4 -Epoch 100	Kokam pouch cells	Room temperature	With other neural network, such as BPNN, ELM, and LSTM	-RMSE 0.58% -MAE 0.47% -MAX 1.32% -R^2 0.9932	More reliable battery datasets can be used for the SOH framework.
SOH [67]	-Number of hidden neurons 256 -Learning rate 0.00001 -Number of epochs 10,000 -Batch size 100	18,650 size li-ion batteries	Room temperature	-With other data-driven models, such as SVR, GPR, GRU, and CNN	For cell 4 -MAE 0.61% -MAX 1.60%	High processing time for model training.

4.3. CNN Framework for SOX Estimation

A CNN model has been employed for delivering outcomes with image recognition and classification. However, the CNN model has been successful in battery SOX estimation too. The CNN model requires low computational training time compared to other neural networks, leading to a decrease in the need for human efforts to develop its functionalities.

4.3.1. CNN-Based SOC Estimation Approaches

Fan et al. [69] presented a SOC estimation approach for lithium-ion batteries by employing a CNN model with a U-net architecture. The public dataset from the Panasonic 18,650 PF cell was employed with a nominal voltage of 3.6 V and nominal capacity of 2.9 Ah. The data collection was conducted based on five different temperatures from 20 °C to 25 °C. The outcomes revealed that an RMSE of 1.4% was achieved at a constant temperature and 1.8% at variable temperatures, respectively. The method was easily executed with satisfactory outcomes; however, validation of the proposed method was not carried out with another model. Cui et al. [70] introduced a CNN-based hybrid model consisting of a CNN and bidirectional weighted GRU (BWGRU). The proposed method limits the influence of battery parameters on the SOC outcomes through a "multi-moment input" structure and bidirectional network. The experimental setup was based on the Mendeley battery dataset which was organized under 12 driving conditions at low temperatures, namely Mixed 1–8, UDDS, HWFET, US06, and LA92. The CNN-BWGRU method was validated with other conventional GRU and CNN-GRU models to demonstrate the effectiveness and accuracy of the proposed model. Further works can be performed to validate the effectiveness of the proposed model based on different temperatures and different aging conditions, respectively. A combined SOC and SOH estimation scheme based on a pruned convolution neural network with a transfer learning model and Gaussian process regression (GPR) was

proposed by Li et al. [71], as shown in Figure 9. Additionally, fiber Bragg grating (FBG) sensors were employed to acquire better process-related signals by connecting them with the battery surface in order to capture the temperature variation due to battery charging and discharging. The proposed work was based on four commercial lithium-ion battery cells with a nominal capacity of 1.6 Ah and nominal voltage of 3.2 V. The SOC estimation with regard to the RMSE and mean standard deviation (MSD) with FBG signals was 3.59% and 1.02%, respectively, and without FBG was 4.3% and 1.77%, respectively. Further research can still be conducted to explore the application of FBG sensors in the state estimation of batteries. Gong et al. [72] developed a novel CNN-based SOC estimation framework for lithium-ion batteries. The data framework for the model training consisting of voltage, current, and temperature sampled in 10 s. The proposed work was conducted based on two public battery datasets from the NASA Ames Research Center and Oxford Battery Degradation dataset. The CNN model operation was evaluated based on different criteria, such as battery datasets and different input lengths. The CNN model for SOC estimation was satisfactory; however, validation with other DL models was not conducted, which could depict more effectiveness of the CNN model.

4.3.2. CNN-Based SOH Estimation Approaches

Li et al. [73] offered a hybrid CNN-LSTM model for SOH and RUL prediction of the lithium-ion BMS applied in EV application, as depicted in Figure 10. The CNN-LSTM model was developed to capture the hierarchical features of several variables associated with temporal dependencies embedded in those features. The battery data features were taken from the battery datasets obtained from NASA. A total of 12 battery datasets were employed for SOH estimation. The training time for the CNN-LSTM model was appropriate and demonstrated high SOH estimation accuracy with a low performance error of 0.0072 for the average RMSE. However, verification and comparative analysis with well-known battery datasets can still be conducted in future research.

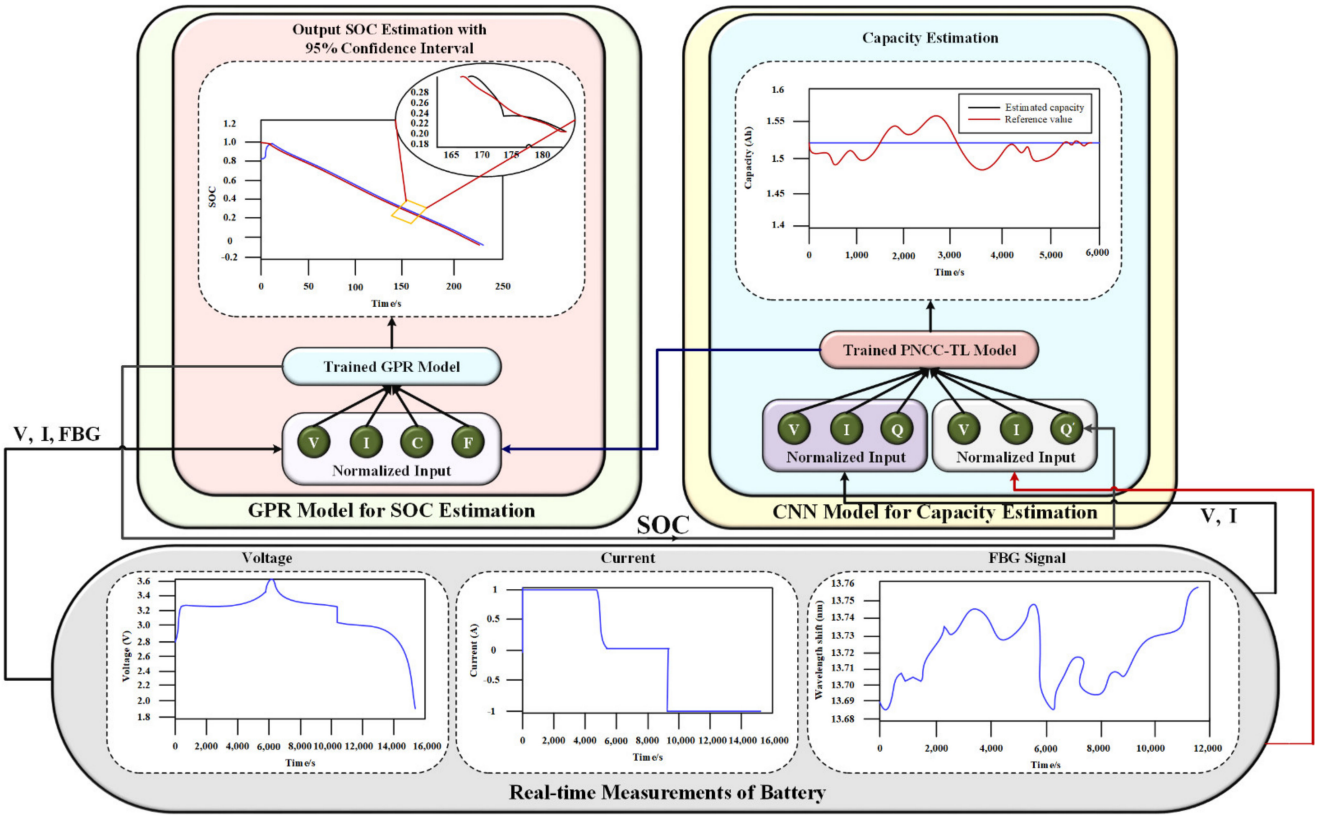

Figure 9. CNN-GPR model-based SOC estimation of lithium-ion battery.

Yang et al. [74] developed a hybrid model combining a CNN and random forest (RF) to predict the SOH of the battery under partial discharge. The extraction of the suitable health indicators correlating with the estimated capacity was executed by the two CNN models, and, consequently, the RF technique was utilized to predict the battery SOH. The experiment was performed considering the MIT battery database which consists of 124 lithium-ion battery datasets. A comparative analysis was performed with RF-ICA, SOH-CNN, and ΔSOH-CNN where the proposed CNN-RF model depicted high robustness and accuracy in SOH prediction. A novel CNN model named the pruned CNN model with transfer learning was explored to predict the SOH of the lithium-ion BMSs [75]. The source and target battery datasets include 16 battery datasets and four battery datasets, respectively. The estimation accuracy was improved by training the proposed pruned CNN model on a large battery dataset and then to the small dataset of the targeted battery by employing the transfer learning technique. The effectiveness of the proposed model was compared to the conventional CNN model and pruned CNN model without the transfer learning technique. The SOH estimation outcomes were satisfactory and achieved a size reduction of 68.34% and a computational saving of 80.97%. The authors in [76] applied a temporal CNN model to capture the phenomena of capacity regeneration and accordingly predict battery SOH. Additionally, the empirical mode decomposition (EMD) technique was employed to denoise the unwanted data affecting the estimation accuracy. The NASA battery datasets and CALCE battery dataset consisting of three batteries were employed for the SOH estimation. The outcomes of CNN-based SOX estimation under various operating conditions are summarized in Table 5.

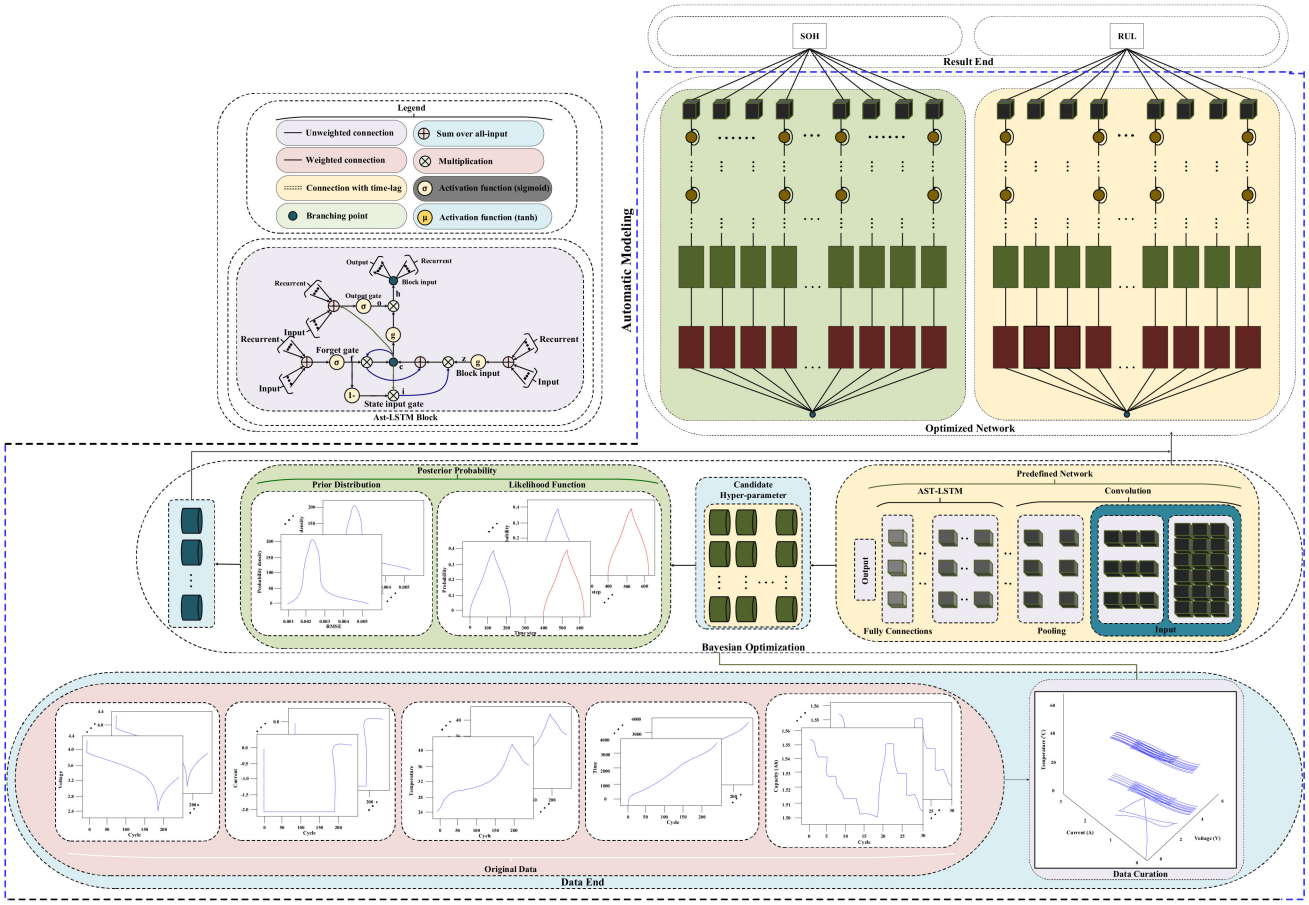

Figure 10. End-to-end prognostic framework of CNN-LSTM based model for SOH and RUL prediction of BMS.

Table 5. Summary of CNN-based SOX estimation approaches.

SOX Estimation	Structure	Battery Chemistry	Thermal Status	Validation Process	Results	Research Gaps
SOC [69]	-Kernel size 5 -U-net depth 3 -Shrink ratio 5-Learning rate 0.001	Panasonic 18,650 PF	5 different temperatures from −20 °C to 25 °C.	With other data-driven models and under different variable temperatures	-RMSE 1.4% (for constant temperature) -RMSE 1.8% (for variable temperature)	Hybridization of the proposed model with appropriate model can be performed for better estimation accuracy
SOC [72]	-Kernel size 1 -Learning rate 0.001 -Number of epochs 1000 -Batch size 32	18,650 lithium-ion batteries	25 °C 40 °C	The validation process was conducted with SRU and CNN-SRU models	For RW13 -RMSE 0.83% -MAE 0.63% -MAXE 5.26% -Time 1.21 s	High computational complexity with more training time
SOH [74]	-Filter size 3 -Filter stride 1 -Convolution filters 50 -Pooling size 3 -Pooling stride 3	lithium–iron-phosphate/graphite cells	Room temperature	With different DoD ranges	For DoD 0.1–0.8 -MAE 0.62%	Validation with other models was not conducted
SOH [76]	-Number of iterations 1000 -Size of the kernel 3 -Mini batch size 128 -Dilation factor [1, 2, 4, 8, 16, 32, 64]	18,650 li-ion batteries	Room temperature	The validation process was conducted with LSTM, CNN, and GRU models	For B0005, start point 30 -RMSE 0.014 -MAE 0.009	Further validation of the model based on different battery chemistries can be explored.

4.4. Autoencoder Framework for SOX Estimation

The autoencoder model is now being utilized in SOX estimation of lithium-ion batteries as it provides the path to reduce the noisy data with ease which makes the DL model more effective for estimation outcomes.

4.4.1. Autoencoder-Based SOC Estimation Approaches

Fasahat and Manthouri [77] developed a SOC estimation technique for lithium-ion batteries by employing a hybrid framework based on autoencoder and LSTM to conduct high-precision estimation. Two driving cycle battery datasets namely the FUDS and DST drive cycle datasets were acquired from three different temperatures (0 °C, 25 °C, and 45 °C). The validation of the autoencoder-LSTM model was conducted with a multi-layer perceptron (MLP) model. It was observed that MAE and MSE for the proposed model at different operating temperatures delivered more accurate outcomes as compared to the MLP model. Further investigation can still be conducted by validating the outcomes of the proposed model with real-time EV drive cycle datasets. Chen et al. [78] presented a hybrid model consisting of an autoencoder and GRU model for SOC estimation of lithium-ion batteries. The denoising autoencoder is used to remove the noise and increase the dimensions of the measured battery data while the GRU model was employed for training and SOC estimation. The dataset obtained to conduct the experiments belongs to the Samsung corporation, Korea consisting of lithium-ion nickel cobalt manganese oxide (NCM) battery. The training operation was conducted with the UDDS driving cycle data while the testing was conducted with the UDDS, HWFET, and NEDS driving cycle data. Additionally, the accuracy of the proposed model was checked with the other methods such as GRU and RNN where the proposed approach delivered accurate outcomes in terms of MAE and RMSE.

4.4.2. Autoencoder-Based SOH Estimation Approaches

Wu et al. [79] introduced an autoencoder and ensemble learning technique based SOH prediction framework, as depicted in Figure 11. The extraction of the critical health features comprising battery charging profiles at different aging stages was conducted by the convolutional autoencoder. Furthermore, an ensemble learning technique was applied to enhance the SOH prediction accuracy of the autoencoder model. The NASA datasets consisting of four battery datasets under different cycling test conditions were used to validate the proposed model. The validation of the autoencoder model was conducted with other models such as conventional GRU and ensemble learning-based GRU models. The outcomes based on RMSE at 1.04% and MAE at 0.77% depicted high SOH estimation

accuracy. However, validation with other battery datasets from the reliable online database should be conducted to enhance the acceptability of the conducted research work.

Sun et al. [80] developed a sparse autoencoder and BPNN-based SOH prediction technique. The input data framework for the model training was conducted by using the battery voltage extracted during the later phase of the charging path. The acquisition of the battery dataset was performed experimentally by conducting the accelerated aging test on 8 batteries with a nominal capacity and nominal voltage of 2500 mAh and 3.2 V, respectively. It was depicted that SOH estimated error was within the range of ±5% which demonstrated the high accuracy and effectiveness of the proposed model with low computational cost. However, further improvements based on the appropriate selection of the model hyperparameters should be undertaken for better estimation accuracy. Son et al. [81] proposed a SOH estimation technique by applying an autoencoder model. The SOH estimation technique consists of three parts namely feature extraction, feature manipulation, and SOH estimation. The feature extraction was performed by the polynomial regression and denoising autoencoder. The SOH prediction was determined by the GPR approach considering the multiple battery health indicators. The autoencoder-based SOH estimation model performance was validated with other models such as SVM, MLP, DCNN, and LSTM methods. The proposed model depicts higher accuracy with the lowest RMSE, however, SOH estimation under the various stochastic operational conditions was not performed. The findings of autoencoder-based SOX estimation under different settings are presented in Table 6.

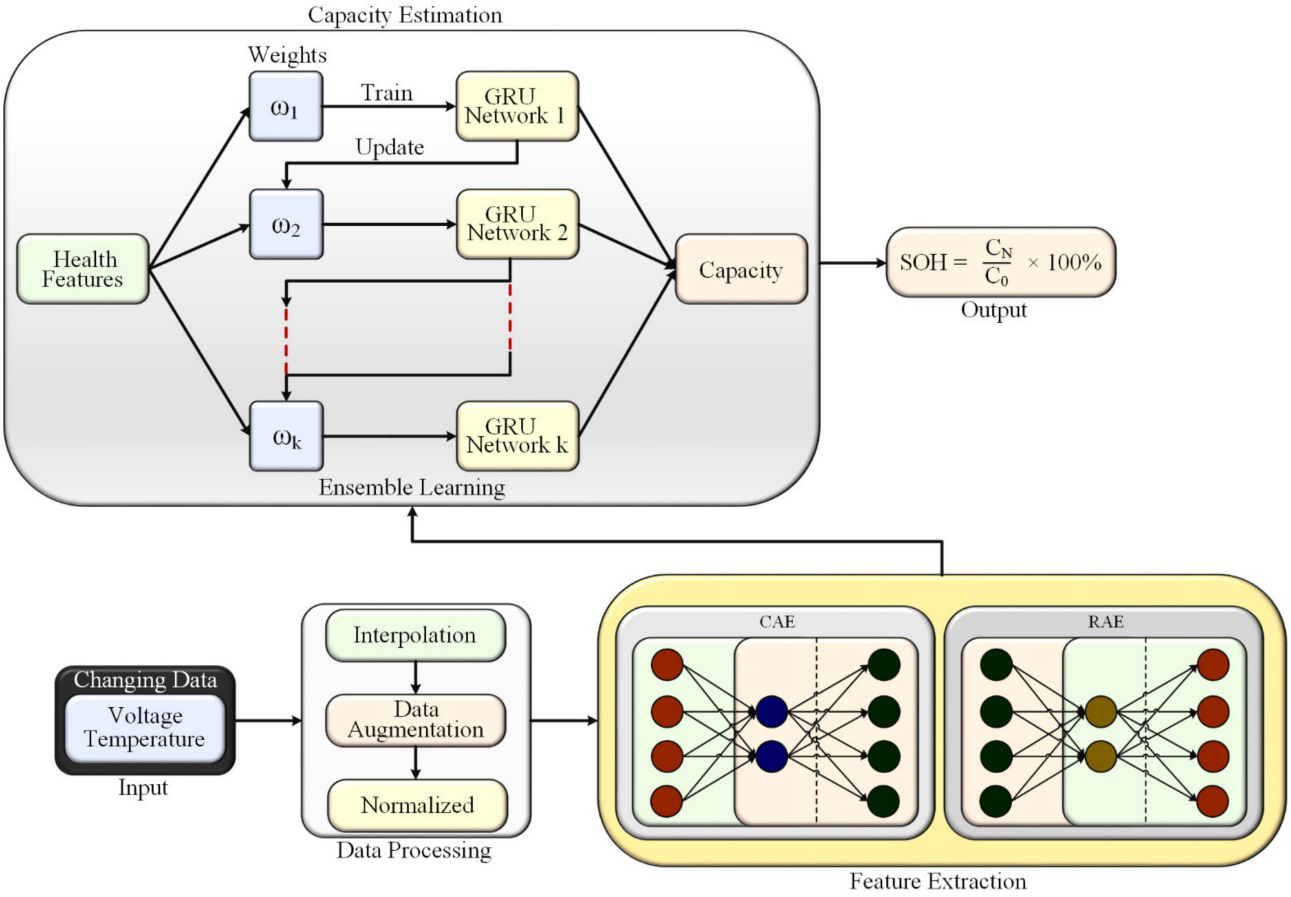

Figure 11. Autoencoder and ensemble learning-based SOH estimation.

Table 6. Summary of autoencoder-based SOX estimation approaches.

SOX Estimation	Structure	Battery Chemistry	Thermal Status	Validation Process	Results	Research Gaps
SOC [78]	-Batch size 64 Training epoch 500 -Learning rate 0.01	NCM battery	Data extraction takes place at 25 °C.	-With other data-driven models and under different testing driving cycle datasets	-RMSE 0.3300 (testing with UDDS) -RMSE 2.1330 (Testing with HWFET)	-Validation with other battery chemistries was not conducted.
SOC [77]	-Hidden layer 1 -Hidden neurons 22	18,650-size lithium-ion Batteries	0, 25, 45 °C	Validation at different temperatures and with conventional MLP model	At 25 °C temperature. -MAE 0.6664 -MSE 1.1886	-Validation with other sophisticated models could have been performed.
SOH [79]	-Encoder 8 layer -Decoder 4 layer	18,650-size lithium-ion batteries	Room Temperature	With another neural network such as LSTM, GPR, and SVM	for B0005: RMSE 0.92% MAE 0.74%	-Effect of temperature profile on capacity degradation can be studied.
SOH [81]	-Encoder 2 layer -Decoder 2 layer -Learning rate 0.001 -Number of epochs 500	$LiFePO_4$ cell	−20 to 60 °C	Validation with data-driven models such as SVM, MLP, DCNN, and LSTM models.	At swelling 15°C: -RMSE 0.003 -RMSE ratio with respect to GPR 1.00	-Validation of the model with another reliable battery database can be conducted.

5. Key Issues and Challenges of DL Applied in Automotive BMS

The use of DL approaches for battery SOX estimation has demonstrated important contributions; however, there are still several internal and external problems and difficulties that need to be resolved. As a result, the main problems and concerns of SOX estimation with DL are roughly categorized into two groups: battery storage issues and methods and execution problems.

5.1. Battery Energy Storage-Related Issues

Due to a number of problems, including battery capacity deterioration, thermal runaway, battery aging, battery materials, and charge balance concerns, the precision of different DL approaches for SOC, SOH, and SOP calculations might differ.

5.1.1. Battery Chemistries and Materials Issues

To test the battery SOX accuracy, Oxford, the National Aeronautics and Space Administration (NASA), and CALCE employed several battery chemistries, materials, and health deterioration profiles. For instance, the Mendeley battery dataset utilized a 1.1 Ah li-ion $LiNiCoAlO_2$ battery whereas CALCE employed a 2.0 Ah li-ion $LiNiMnCoO_2$ battery [82]. The use of various li-ion battery chemistries may affect the accuracy of DL techniques. A GRU-dependent DL approach for SOC prediction utilizing lithium-iron phosphate (Li-FP) and Li-NMC cells was developed by Yang et al. [83]. According to the findings, the MAE and RMSE of the Li-NMC battery were less than the Li-PF cell. The accuracy of the SOC estimation approach was examined in [84] by using two distinct lithium-ion battery chemistries. An aging cycle test and a test bench platform were used for validation. The trials were first carried out using brand-new lithium-ion battery cells, and it was found that the $LiFePO_4$ battery performed more accurately than the LTO battery with an RMSE of 0.5305% at 25 °C. The LTO battery demonstrated improved results in the aging cycle test. Therefore, more investigation is necessary to ensure the accuracy of DL approaches when used with various li-ion battery materials.

5.1.2. Battery Aging Characterizes

The issue of battery aging is another major factor in the deterioration of the precision. Of DL techniques. According to previous research, acceleration of the aging cycle results in a number of issues, including the deterioration of cathode materials, that reduce the estimation accuracy of DL methods. Several important studies employing ML approaches for SOC estimate in battery aging have been conducted. For example, Chaoui et al. [85] used an RNN algorithm to conduct an aging estimation for the SOC of $LiFePO_4$ batteries. The findings demonstrated that when the battery aged to 10% of its fundamental capacity,

the RMSE of the SOC increased to 2.7×10^{-3}% from 1.9×10^{-3}%. Han et al. [86] conducted a thorough analysis of the main problems with battery deterioration across the whole life cycle. To better comprehend the battery fade characteristic, the internal aging mechanisms of the battery were first evaluated while taking into account various anode and cathode materials. The influencing elements affecting battery life were then thoroughly examined from the viewpoints of design, production, and application in order to achieve improved life performance. DL techniques under the aging cycle, however, have not yet been investigated. Therefore, to estimate battery SOX accurately, battery aging is a crucial topic that requires additional consideration.

5.1.3. Battery Thermal Issue

When evaluating the effectiveness of various DL algorithms for SOX estimation, battery temperature is a key factor. When temperatures alter, the accuracy of SOX is affected. For instance, SOC-based GRU under various temperature conditions was examined by Yang et al. [63]. The findings exhibited that the performance of the training model was affected by the temperature fluctuating between 0–50 °C, leading to a change in the RMSE between 1.81% and 2.33%. Likewise, Mamo et al. [51] investigated the effects of temperature on the SOC utilizing LSTM and found that the RMSE was estimated to be 0.95%, 0.87%, and 0.92% at 0 °C, 25 °C, and 45 °C, respectively. In contrast to conventional li-ion batteries, $LiFePO_4$ has a restricted exothermic heat discharge, which improves thermal stability [87]. According to Wang et al. [88], when the battery temperature increases by 1 °C, the battery's lifespan reduces by two months. In order to build an appropriate heating and cooling system for BMSs, additional exploration is necessary to understand heat management in the battery systems of EVs. Therefore, extensive research is needed to verify the performance of SOX at various temperatures.

5.1.4. Battery Balancing and Cell Inconsistency Concerns

Battery overcharging and undercharging issues originate from battery charge imbalances and cell inconsistencies. Additionally, battery charge imbalances are observed as a result of age, manufacturing standards, material flaws, capacity changes, and changes in physical features [89]. Charge imbalance is also frequently reported in much of the literature. A study by Park et al. [90] used LSTM and DNN approaches to calculate the SOC of a battery pack made up of four lithium-ion battery cells. Due to the restriction of weakening cells, passive balancing was ineffective when batteries were drained [91]. Because active balancing redistributes energy across cells rather than squandering it and dissipating it, it is both required and more effective at balancing the energy of a cell. Therefore, an intelligent system must be created to address the problems caused by charge imbalance in the SOP, SOH, SOE, and SOC prediction processes in BMSs.

5.2. DL Methods and Operation Problems

This section discusses numerous operational concerns of DL algorithms, including factors and optimum DL approach selection.

5.2.1. DL Algorithm Execution Concerns

Even while the use of DL algorithms for BMSs in EVs has shown encouraging results, it still has certain drawbacks. For instance, in time series prediction, LSTM can retain all information throughout time; however, it has flaws, such as explosion and gradient vanishing. Although LSTM does not need fine-tuning of characteristics such as learning rates, it takes a longer time. Apart from this, GRU performs admirably in terms of memory use and quick computing speed, but its accuracy is hampered when employing lengthy sequences. Although CNN demonstrates effectiveness when using pooling and convolution methods for factor sharing, it needs a large volume of data for smooth functioning. Autoencoders offer a number of filters to minimize the dimensional issues but demand a huge volume of data, a powerful computer, and hyperparameter adjustment.

5.2.2. Quantity and Quality of Data

The precise quality and quantity of data are essential in the effectiveness and accuracy of a DL approach. For instance, a low data volume reduces a DL algorithm's accuracy whereas a high data volume results in a significant computational cost and additional overfitting concerns [92]. It requires a great amount of time and effort to gather a lot of data over a period of time. Additionally, there are differences in data for distinct EV cycles with different current and voltage value patterns. Additionally, the EV driving cycle is repeated multiple times to gather a significant amount of training dataset [93]. Although a big data set can produce superior results, the longer training period and increased computing load cause overfitting issues [92]. Therefore, it is crucial to take into account the issue of data quantity and quality.

5.2.3. Higher Computational Cost and Complexity

The precision and length of training, especially for deep learning algorithms, provide one of the main obstacles to the successful use of intelligent approaches. Chemali et al. [27] trained DL approaches offline using tens of thousands of battery data points over the course of 50–60 h [94]. The efficiency of the computational cost determines whether a DL approach is appropriate for a real-time BMS. The effectiveness of different DL algorithms in terms of computing varies. Certain research recommends GeForce GTX 1080 Ti and NVIDIA GeForce GTX 1070 Ti to determine SOX [56,67,95]. However, as dataset volumes grow and configurations get more complicated with more hidden layers, computing costs and complexity rise. In order to implement SOX through onboard-BMSs with minimal storage and power requirements, additional research is necessary.

5.2.4. Appropriate Functions and Parameters Selection

To increase efficiency and accuracy, it is important to choose proper training settings for DL methods. The accuracy of DL approaches is influenced by the selection of appropriate training and activation functions. Additionally, computation issues are decreased by properly choosing hyperparameters for DL algorithms [39]. Hyperparameters are typically tuned using the TE method until acceptable results are obtained. However, TE illustrates a significant loss of human energy and time. Therefore, more research is required to train DL approaches by choosing appropriate hyperparameters.

5.2.5. Difficulties in Executing Optimized DL Methods

The accuracy, robustness, and efficiency of SOX for online BMS applications have recently been improved by the deployment of several optimization schemes, including a lighting search algorithm (LSA) [96], gravitational search algorithm (GSA) [25], backtracking search algorithm (BSA) [97], particle swarm optimization (PSO) [98], etc. However, each optimization technique has a unique learning execution time, convergence, and accuracy. Additionally, the development of optimization includes a number of parameters and operational steps that not only call for intensive training and human expertise but also result in a significant computing burden. To improve the accuracy of SOX, more research is required on the integration of appropriate optimization techniques with DL methodologies.

5.2.6. Missing Regular/Irregular Data in Real-World Applications

Typically, the data derived from laboratory studies provide good results; however, the data gathered from the outside world shows less accurate performance. The absence of data in predictable or unpredictable patterns is the cause of the reduced estimation accuracy [99]. There are a number of methods that may be applied to deal with the problems caused by missing or irregular data. It is possible to include regularly sampled data in some circumstances whereas irregular data are interpolated in other circumstances [100]. Additionally, a signal processing-based method can be used for data interpolation. Fast generalized Fourier transform (FGFT) may use to do the data interpolation. However,

further research is required to make up for the missing data inconsistencies and achieve enhanced performance in real-world scenarios.

5.2.7. Validation Complexities under Real-World Data

One of the obstacles to implementing DL techniques with real-world data is data integrity. Some research establishments have published high-quality battery datasets based on different experimental conditions. The dataset comprises charging and discharging battery current and EV drive cycles following specific procedures and requirements. The battery datasets were acquired from various experimental conditions based on different charge/discharge current rates under varying temperature conditions. Furthermore, the battery parameter profiles of current and voltage for the EV drive cycle do not match with actual data in real-world applications. Therefore, further investigation needs to be performed for delivering and validating complex, real-world data.

5.2.8. Joint Estimation of SOE, SOH, SOP, and SOC Estimation

A multiscale and joint estimation technique may be used to minimize the calculations of BMSs for SOE, SOH, SOP, and SOC prediction depending on deep learning approaches. While the RUL and SOH are tracked with variations in battery capacities, the SOC is examined with current level changes. Battery currents fluctuate a lot, and battery capacities decrease as they ages. As a result, multiple time frames are needed for the monitoring of a battery's various states. Additionally, the majority of research papers have focused on single estimations, such as RUL, SOP, SOE, and SOC. However, only a small number of prominent papers have concentrated on the application of DL techniques for multiple measurements together although Cui and Hu [57] presented LSTM for the combined measurement of RUL and SOH of li-ion batteries. Apart from this, Li et al. [56] proposed a unique LSTM approach for estimating RUL and SOH concurrently. To overcome the abovementioned issues, further exploration is required.

6. Conclusions and Future Research Opportunities

This paper outlines various DL approaches and frameworks for SOX estimation for BMSs in EV applications. SOX in terms of SOE, SOH, and SOC is extensively explored employing LSTM, GRU, CNNs, and autoencoders. As a first contribution, various DL techniques for SOX estimation were comprehensively reviewed in terms of methods, operation, mathematical expressions, advantages, and disadvantages. As a second contribution, several important aspects and factors were investigated, including configuration, parameters, battery types, temperature status, validation profiles, accuracy, benefits, drawbacks, and research gasps. As a third contribution, numerous key issues and limitations for DL-based SOX estimation were delivered with regard to battery materials, algorithm complexities, and validation difficulties. Fourthly, future aspects and suggestions for SOX estimation were discussed. This analysis reveals that DL-based SOX estimation achieves excellent outcomes under various battery chemistries, varying temperature conditions, and different validation processes. Moreover, this survey denotes the limitations, issues, and challenges in determining the SOX of BMSs, covering battery-related problems, algorithm execution difficulties, and operational constraints. The investigation discloses that battery materials, aging, thermal degradation, charge balancing, data amount, data quality, computational cost, activation functions, and hyperparameters play a crucial role in achieving accurate and robust SOX estimation. Finally, this paper delivers several effective and productive recommendations for future research opportunities which are mentioned below.

- Primarily, the extraction of the data samples was performed by utilizing an advanced battery testing system (BTS), such NEWARE BTS 4000, DAQ, Arbin BT 2000, and Digatron. However, the acquired data samples consist of inaccurate data samples because of the involvement of electromagnetic interference (EMI), noise influence, and equipment accuracy. Additionally, the precise justification of the SOX methods may not be conducted due to sensor inaccuracies and EMI. Therefore, it is vital to

develop a BTS for accurate data extraction for developing a SOX estimation framework. Considering this, some techniques associated with noise reduction, such as recursive total least squares, bias compensating, a Butterworth filter, and a wavelength transform method, can be applied.

- The framework associated with hybrid models of SOX estimation has been effective with the accurate estimation of outcomes compared to single model estimation accuracy. Usually, a hybrid model is developed based on the association amongst a PF-based technique, KF-based technique, and data-driven-based models [47]. Nonetheless, the inaccurate hybridization of two or more models for SOX estimation may result in computational burden, data overfitting, and inaccurate estimation outcomes. Therefore, an appropriate study should be conducted, and practical feasibility should be studied for hybridizing models for SOX estimation.
- Usually, SOX estimation is conducted based on data acquired from a single battery cell. However, the BMS structure consists of several battery cells connected in series and parallel. When battery cells are connected in series and parallel, unbalancing issues are observed due to continuous charging and discharging. Due to this, the estimation accuracy of the battery pack is not the same or as accurate as the estimation with a single battery cell. To overcome the issue, various converters and controllers have been modeled to reduce the abovementioned challenges. Additionally, relevant investigations associated with reducing the size, expenses, equalization time, voltage and current stress, power loss, and efficiency should be conducted.
- The execution of DL models for the SOX estimation of the lithium-ion battery takes significant time for model training and delivering estimation outcomes. DL model training time can be appropriately reduced with suitable selection of model hyperparameters considering the estimation outcomes as well. Currently, complex DL models are executed in advanced GPU technologies, such as GeForce GTX 1080Ti and NVIDIA GeForce GTX 1070Ti, to accelerate SOX estimation.
- An accurate SOX estimation can be obtained with suitable selection of the model hyperparameters. When the selection of model hyperparameters, such as hidden neurons, number of iterations, epochs, activation function, bias, and weight, is not appropriate, the computational burden is increased, and issues associated with data overfitting and data underfitting occur. Generally, the model hyperparameters are selected based on the TE method which requires human expertise and is time consuming. Therefore, appropriate execution of the metaheuristic optimization technique can be implemented along with DL models for the suitable selection of model hyperparameters. Therefore, execution of optimization techniques in SOX estimation frameworks should be further explored.
- Currently, SOX estimations are performed under a preset environmental condition. However, the application of cloud computing and the internet of things (IoT) platform for online SOX estimation has not been investigated properly. The integration of the IoT-based platform with SOX estimation frameworks will be beneficial with a large volume of data acquired in real-time implementation along with accurate SOX estimation. Maddikunta et al. [101] developed a predictive model for battery life estimation in the internet of things (IoT) platform. Automated data sensors were employed to access the data while data preprocessing methods, such as normalization and transformation, were used. The outcomes were satisfactory with an accuracy of 95%.
- However, research based on the execution of IoT-based real-time implementation for SOX application has not been significantly explored, and, therefore, further research should be conducted to explore the possibilities of integrating SOX estimation with IoT.
- The computational complication and burden of SOX estimation can be improved with the application of multiscale and joint estimation processes. However, it should be studied that each SOX estimation is conducted based on different conditions, such as the SOC, which is conducted with the change in current values while the

SOH is estimated based on battery capacity. There is frequent change in battery currents whereas battery capacities age with battery cycles. Therefore, every battery state estimation requires different time scales, which should be explored for the development of an accurate joint estimation framework.

The critical discussion, analysis, key findings, issues, and future suggestions would provide important guidelines to automotive engineers and industries to design an improved SOX estimation framework using various DL approaches. Intelligent BMSs with DL approaches to estimate accurate SOX estimation will enhance battery performance as well as EV safety and reliability toward low carbon energy transitions in the future.

Author Contributions: Conceptualization, M.S.H.L. and T.F.K.; methodology, M.S.H.L.; formal analysis, M.S.H.L.; investigation, M.S.H.L.; writing—original draft preparation, M.S.H.L., T.F.K., S.A. and M.S.M. writing—review and editing, S.T.M., R.M.E. and R.R.V.; visualization, M.S.R.; supervision, M.S.H.L.; project administration, M.S.H.L.; funding acquisition, R.M.E. All authors have read and agreed to the published version of the manuscript.

Funding: This research received no external funding.

Acknowledgments: The authors acknowledge the Green University of Bangladesh for conducting this research work.

Conflicts of Interest: The authors declare no conflict of interest.

Abbreviations

BGRU	Bidirectional GRU
BO	Bayesian optimization
BSA	Backtracking search algorithm
BTS	Battery testing system
BWGRU	Bidirectional weighted GRU
CALCE	Center for Advanced Life Cycle Engineering
CDTL	Controllable deep transfer learning
CNN	Convolutional Neural Network
DEGWO	Differential evolution grey wolf optimizer
DFFNN	Deep feedforward neural network
DL	Deep learning
DST	Dynamic stress testing
EMI	Electromagnetic interference
EV	Electric vehicle
FBG	Fiber Bragg grating
FFNN	Feedforward neural network
FGFT	Fast generalized Fourier transform
FUDS	Federal urban driving schedule
GPR	Gaussian process regression
GPU	Graphics processing unit
GSA	Gravitational search algorithm
IoT	Internet of things
LFP	Lithium iron phosphate/graphite
Li-FP	Li-iron phosphate
LSA	Lighting search algorithm
LSTM	Long short-term memory
LTO	Lithium titanate
MAE	Mean absolute error
MSE	Mean squared error
MLP	Multilayer perceptron
NASA	National Aeronautics and Space Administration
NCM	Nickel cobalt manganese oxide
PSO	Particle swarm optimized

RMSE	Root mean square error
RUL	Remaining useful life
SOC	State of charge
SOE	State of energy
SOH	State of health
TE	Trial and error
VLSTM	Variant long short-term memory
UDDS	Urban Dynamometer Driving Schedule

Symbols

σ ()	Sigmoid activation function
A	Input data dimension
B	Refers to padding
$B_i^{(l)}$	Bias matrix
b_f	Bias vector of forget gate
b_i, b_c	Input gates
b_o	Bias vector of output gate
C	Dimension of filter
D	Stride
f'	Encoder
f_k	Forget gate
g'	Decoder
h_m	Feature vector
$k_{i,j}^{(l)}$	Filter of size $2h_1^{(l)} + 1 * 2h_2^{(l)} + 1$
o_k	Output gate
r_t	Reset gate
W_o	Weight matrix
W_f	Weight matrix of the forgot gate
W_i, W_c	Weight matrix of the input gate
W_z	Weight matrix of the update gate
$W_{i,j,r,s}^{(l)}$	Connection of weight position
x_m	Unlabeled data
x'_m	Reconstructed unlabeled data
x_k	Current time step of input k
z_t	Update gate
$tanh$	Activation function

References

1. Lipu, M.S.H.; Hannan, M.A.; Karim, T.F.; Hussain, A.; Saad, M.H.M.; Ayob, A.; Miah, M.S.; Mahlia, T.M.I. Intelligent algorithms and control strategies for battery management system in electric vehicles: Progress, challenges and future outlook. *J. Clean. Prod.* **2021**, *292*, 126044. [CrossRef]
2. Tu, R.; Gai, Y.J.; Farooq, B.; Posen, D.; Hatzopoulou, M. Electric vehicle charging optimization to minimize marginal greenhouse gas emissions from power generation. *Appl. Energy* **2020**, *277*, 115517. [CrossRef]
3. Pavić, I.; Pandžić, H.; Capuder, T. Electric vehicle based smart e-mobility system—Definition and comparison to the existing concept. *Appl. Energy* **2020**, *272*, 115153. [CrossRef]
4. Rietmann, N.; Hügler, B.; Lieven, T. Forecasting the trajectory of electric vehicle sales and the consequences for worldwide CO_2 emissions. *J. Clean. Prod.* **2020**, *261*, 121038. [CrossRef]
5. Zhang, J.; Wang, Z.; Liu, P.; Zhang, Z. Energy consumption analysis and prediction of electric vehicles based on real-world driving data. *Appl. Energy* **2020**, *275*, 115408. [CrossRef]
6. Jaguemont, J.; Boulon, L.; Dubé, Y. A comprehensive review of lithium-ion batteries used in hybrid and electric vehicles at cold temperatures. *Appl. Energy* **2016**, *164*, 99–114. [CrossRef]
7. Gandoman, F.H.; Firouz, Y.; Hosen, M.S.; Kalogiannis, T.; Jaguemont, J.; Berecibar, M.; van Mierlo, J. Reliability assessment of NMC li-ion battery for electric vehicles application. In Proceedings of the 2019 IEEE Vehicle Power and Propulsion Conference (VPPC), Hanoi, Vietnam, 14–17 October 2019. [CrossRef]
8. Xiong, R.; Sun, W.; Yu, Q.; Sun, F. Research progress, challenges and prospects of fault diagnosis on battery system of electric vehicles. *Appl. Energy* **2020**, *279*, 115855. [CrossRef]

9. Xiong, R.; Pan, Y.; Shen, W.; Li, H.; Sun, F. Lithium-ion battery aging mechanisms and diagnosis method for automotive applications: Recent advances and perspectives. *Renew. Sustain. Energy Rev.* **2020**, *131*, 110048. [CrossRef]
10. Zhao, G.; Wang, X.; Negnevitsky, M.; Zhang, H. A review of air-cooling battery thermal management systems for electric and hybrid electric vehicles. *J. Power Source* **2021**, *501*, 230001. [CrossRef]
11. Su, S.; Li, W.; Li, Y.; Garg, A.; Gao, L.; Zhou, Q. Multi-objective design optimization of battery thermal management system for electric vehicles. *Appl. Therm. Eng.* **2021**, *196*, 117235. [CrossRef]
12. Lipu, M.S.H.; Miah, M.S.; Ansari, S.; Wali, S.B.; Jamal, T.; Elavarasan, R.M.; Kumar, S.; Ali, M.M.N.; Sarker, M.R.; Aljanad, A.; et al. Smart Battery Management Technology in Electric Vehicle Applications: Analytical and Technical Assessment toward Emerging Future Directions. *Batteries* **2022**, *8*, 219. [CrossRef]
13. Xiong, R.; Li, L.; Tian, J. Towards a smarter battery management system: A critical review on battery state of health monitoring methods. *J. Power Source* **2018**, *405*, 18–29. [CrossRef]
14. Wang, Y.; Tian, J.; Sun, Z.; Wang, L.; Xu, R.; Li, M.; Chen, Z. A comprehensive review of battery modeling and state estimation approaches for advanced battery management systems. *Renew. Sustain. Energy Rev.* **2020**, *131*, 110015. [CrossRef]
15. Ayob, A.; Ansari, S.; Lipu, M.S.H.; Hussain, A.; Saad, M.H.M. SOC, SOH and RUL Estimation for Supercapacitor Management System: Methods, Implementation Factors, Limitations and Future Research Improvements. *Batteries* **2022**, *8*, 189. [CrossRef]
16. Hu, X.; Feng, F.; Liu, K.; Zhang, L.; Xie, J.; Liu, B. State estimation for advanced battery management: Key challenges and future trends. *Renew. Sustain. Energy Rev.* **2019**, *114*, 109334. [CrossRef]
17. Xiao, D.; Fang, G.; Liu, S.; Yuan, S.; Ahmed, R.; Habibi, S.; Emadi, A. Reduced-Coupling Coestimation of SOC and SOH for Lithium-Ion Batteries Based on Convex Optimization. *IEEE Trans. Power Electron.* **2020**, *35*, 12332–12346. [CrossRef]
18. Shen, P.; Ouyang, M.; Lu, L.; Li, J.; Feng, X. The co-estimation of state of charge, state of health, and state of function for lithium-ion batteries in electric vehicles. *IEEE Trans. Veh. Technol.* **2018**, *67*, 92–103. [CrossRef]
19. Feng, F.; Teng, S.; Liu, K.; Xie, J.; Xie, Y.; Liu, B.; Li, K. Co-estimation of lithium-ion battery state of charge and state of temperature based on a hybrid electrochemical-thermal-neural-network model. *J. Power Source* **2020**, *455*, 227935. [CrossRef]
20. Zeng, M.; Zhang, P.; Yang, Y.; Xie, C.; Shi, Y. SOC and SOH Joint Estimation of the Power Batteries Based on Fuzzy Unscented Kalman Filtering Algorithm. *Energies* **2019**, *12*, 3122. [CrossRef]
21. Ali, M.U.; Zafar, A.; Nengroo, S.H.; Hussain, S.; Alvi, M.J.; Kim, H.-J. Towards a Smarter Battery Management System for Electric Vehicle Applications: A Critical Review of Lithium-Ion Battery State of Charge Estimation. *Energies* **2019**, *12*, 446. [CrossRef]
22. Xu, C.; Cleary, T.; Wang, D.; Li, G.; Rahn, C.; Wang, D.; Rajamani, R.; Fathy, H.K. Online state estimation for a physics-based Lithium-Sulfur battery model. *J. Power Source* **2021**, *489*, 229495. [CrossRef]
23. Ren, L.; Zhu, G.; Kang, J.; Wang, J.V.; Luo, B.; Chen, C.; Xiang, K. An algorithm for state of charge estimation based on a single-particle model. *J. Energy Storage* **2021**, *39*, 102644. [CrossRef]
24. Li, S.; Li, Y.; Zhao, D.; Zhang, C. Adaptive state of charge estimation for lithium-ion batteries based on implementable fractional-order technology. *J. Energy Storage* **2020**, *32*, 101838. [CrossRef]
25. Lipu, M.S.H.; Hannan, M.A.; Hussain, A.; Saad, M.H.; Ayob, A.; Uddin, M.N. Extreme learning machine model for state-of-charge estimation of lithium-ion battery using gravitational search algorithm. *IEEE Trans. Ind. Appl.* **2019**, *55*, 4225–4234. [CrossRef]
26. Sahinoglu, G.O.; Pajovic, M.; Sahinoglu, Z.; Wang, Y.; Orlik, P.V.; Wada, T. Battery State-of-Charge Estimation Based on Regular/Recurrent Gaussian Process Regression. *IEEE Trans. Ind. Electron.* **2018**, *65*, 4311–4321. [CrossRef]
27. Chemali, E.; Kollmeyer, P.J.; Preindl, M.; Emadi, A. State-of-charge estimation of Li-ion batteries using deep neural networks: A machine learning approach. *J. Power Source* **2018**, *400*, 242–255. [CrossRef]
28. Yang, F.; Song, X.; Xu, F.; Tsui, K.L. State-of-Charge Estimation of Lithium-Ion Batteries via Long Short-Term Memory Network. *IEEE Access* **2019**, *7*, 53792–53799. [CrossRef]
29. Lipu, M.S.H.; Ansari, S.; Miah, M.S.; Meraj, S.T.; Hasan, K.; Shihavuddin, A.S.M.; Hannan, M.A.; Muttaqi, K.M.; Hussain, A. Deep learning enabled state of charge, state of health and remaining useful life estimation for smart battery management system: Methods, implementations, issues and prospects. *J. Energy Storage* **2022**, *55*, 105752. [CrossRef]
30. Li, C.; Wang, Z. The local discontinuous Galerkin finite element methods for Caputo-type partial differential equations: Numerical analysis. *Appl. Numer. Math.* **2019**, *140*, 1–22. [CrossRef]
31. Gao, Y.; Xiang, X.; Xiong, N.; Huang, B.; Lee, H.J.; Alrifai, R.; Jiang, X.; Fang, Z. Human Action Monitoring for Healthcare Based on Deep Learning. *IEEE Access* **2018**, *6*, 52277–52285. [CrossRef]
32. Li, Y.; Liu, D.; Li, H.; Li, L.; Li, Z.; Wu, F. Learning a Convolutional Neural Network for Image Compact-Resolution, IEEE Trans. *Image Process* **2019**, *28*, 1092–1107. [CrossRef] [PubMed]
33. Kadetotad, D.; Yin, S.; Berisha, V.; Chakrabarti, C.; Seo, J.S. An 8.93 TOPS/W LSTM Recurrent Neural Network Accelerator Featuring Hierarchical Coarse-Grain Sparsity for On-Device Speech Recognition. *IEEE J. Solid-State Circuits* **2020**, *55*, 1877–1887. [CrossRef]
34. Farmann, A.; Waag, W.; Marongiu, A.; Sauer, D.U. Critical review of on-board capacity estimation techniques for lithium-ion batteries in electric and hybrid electric vehicles. *J. Power Source* **2015**, *281*, 114–130. [CrossRef]
35. Shrivastava, P.; Soon, T.K.; Idris, M.Y.I.B.; Mekhilef, S. Overview of model-based online state-of-charge estimation using Kalman filter family for lithium-ion batteries. *Renew. Sustain. Energy Rev.* **2019**, *113*, 109233. [CrossRef]
36. Tian, H.; Kong, G.; Wu, Y. Dual feature extractor generative adversarial network for colorization. *J. Electron. Imaging* **2020**, *29*, 043001. [CrossRef]

37. How, D.N.T.; Hannan, M.A.; Lipu, M.S.H.; Ker, P.J. State of Charge Estimation for Lithium-Ion Batteries Using Model-Based and Data-Driven Methods: A Review. *IEEE Access* **2019**, *7*, 136116–136136. [CrossRef]
38. Li, Y.; Liu, K.; Foley, A.M.; Zülke, A.; Berecibar, M.; Nanini-Maury, E.; van Mierlo, J.; Hoster, H.E. Data-driven health estimation and lifetime prediction of lithium-ion batteries: A review. *Renew. Sustain. Energy Rev.* **2019**, *113*, 109254. [CrossRef]
39. Lipu, M.S.H.; Hannan, M.A.; Hussain, A.; Ayob, A.; Saad, M.H.M.; Karim, T.F.; How, D.N.T. Data-driven state of charge estimation of lithium-ion batteries: Algorithms, implementation factors, limitations and future trends. *J. Clean. Prod.* **2020**, *277*, 124110. [CrossRef]
40. Lipu, M.S.H.; Hannan, M.A.; Hussain, A.; Hoque, M.M.; Ker, P.J.; Saad, M.H.M.; Ayob, A. A review of state of health and remaining useful life estimation methods for lithium-ion battery in electric vehicles: Challenges and recommendations. *J. Clean. Prod.* **2018**, *205*, 115–133. [CrossRef]
41. Hannan, M.A.; Hoque, M.M.; Hussain, A.; Yusof, Y.; Ker, P.J. State-of-the-Art and Energy Management System of Lithium-Ion Batteries in Electric Vehicle Applications: Issues and Recommendations. *IEEE Access* **2018**, *6*, 19362–19378. [CrossRef]
42. Yang, S.; Zhang, C.; Jiang, J.; Zhang, W.; Zhang, L.; Wang, Y. Review on state-of-health of lithium-ion batteries: Characterizations, estimations and applications. *J. Clean. Prod.* **2021**, *314*, 128015. [CrossRef]
43. Zhang, R.; Xia, B.; Li, B.; Cao, L.; Lai, Y.; Zheng, W.; Wang, H.; Wang, W.; Wang, M. A Study on the Open Circuit Voltage and State of Charge Characterization of High Capacity Lithium-Ion Battery Under Different Temperature. *Energies* **2018**, *11*, 2408. [CrossRef]
44. Berecibar, M.; Gandiaga, I.; Villarreal, I.; Omar, N.; van Mierlo, J.; van den Bossche, P. Critical review of state of health estimation methods of Li-ion batteries for real applications. *Renew. Sustain. Energy Rev.* **2016**, *56*, 572–587. [CrossRef]
45. Vidal, C.; Malysz, P.; Kollmeyer, P.; Emadi, A. Machine Learning Applied to Electrified Vehicle Battery State of Charge and State of Health Estimation: State-of-the-Art. *IEEE Access* **2020**, *8*, 52796–52814. [CrossRef]
46. Jordan, M.I.; Mitchell, T.M. Machine learning: Trends, perspectives, and prospects. *Science* **2015**, *349*, 255–260. [CrossRef]
47. Ansari, S.; Ayob, A.; Lipu, M.S.H.; Hussain, A.; Saad, M.H.M. Remaining useful life prediction for lithium-ion battery storage system: A comprehensive review of methods, key factors, issues and future outlook. *Energy Rep.* **2022**, *8*, 12153–12185. [CrossRef]
48. Chen, J.; Zhang, Y.; Wu, J.; Cheng, W.; Zhu, Q. SOC estimation for lithium-ion battery using the LSTM-RNN with extended input and constrained output. *Energy* **2023**, *262*, 125375. [CrossRef]
49. Almaita, E.; Alshkoor, S.; Abdelsalam, E.; Almomani, F. State of charge estimation for a group of lithium-ion batteries using long short-term memory neural network. *J. Energy Storage* **2022**, *52*, 104761. [CrossRef]
50. Oyewole, I.; Chehade, A.; Kim, Y. A controllable deep transfer learning network with multiple domain adaptation for battery state-of-charge estimation. *Appl. Energy* **2022**, *312*, 118726. [CrossRef]
51. Takyi-Aninakwa, P.; Wang, S.; Zhang, H.; Li, H.; Xu, W.; Fernandez, C. An optimized relevant long short-term memory-squared gain extended Kalman filter for the state of charge estimation of lithium-ion batteries. *Energy* **2022**, *260*, 120043. [CrossRef]
52. Ren, X.; Liu, S.; Yu, X.; Dong, X. A method for state-of-charge estimation of lithium-ion batteries based on PSO-LSTM. *Energy* **2021**, *234*, 121236. [CrossRef]
53. Ma, Y.; Shan, C.; Gao, J.; Chen, H. A novel method for state of health estimation of lithium-ion batteries based on improved LSTM and health indicators extraction. *Energy* **2022**, *251*, 123973. [CrossRef]
54. Gong, Y.; Zhang, X.; Gao, D.; Li, H.; Yan, L.; Peng, J.; Huang, Z. State-of-health estimation of lithium-ion batteries based on improved long short-term memory algorithm. *J. Energy Storage* **2022**, *53*, 105046. [CrossRef]
55. He, Z.; Shen, X.; Sun, Y.; Zhao, S.; Fan, B.; Pan, C. State-of-health estimation based on real data of electric vehicles concerning user behavior. *J. Energy Storage* **2021**, *41*, 102867. [CrossRef]
56. Li, P.; Zhang, Z.; Xiong, Q.; Ding, B.; Hou, J.; Luo, D.; Rong, Y.; Li, S. State-of-health estimation and remaining useful life prediction for the lithium-ion battery based on a variant long short term memory neural network. *J. Power Source* **2020**, *459*, 228069. [CrossRef]
57. Cui, X.; Hu, T. State of Health Diagnosis and Remaining Useful Life Prediction for Lithium-ion Battery Based on Data Model Fusion Method. *IEEE Access* **2020**, *8*, 207298–207307. [CrossRef]
58. Wu, J.; Zhang, C.; Chen, Z. An online method for lithium-ion battery remaining useful life estimation using importance sampling and neural networks. *Appl. Energy* **2016**, *173*, 134–140. [CrossRef]
59. Wu, Y.; Xue, Q.; Shen, J.; Lei, Z.; Chen, Z.; Liu, Y. State of Health Estimation for Lithium-Ion Batteries Based on Healthy Features and Long Short-Term Memory. *IEEE Access* **2020**, *8*, 28533–28547. [CrossRef]
60. Fan, T.E.; Liu, S.M.; Tang, X.; Qu, B. Simultaneously estimating two battery states by combining a long short-term memory network with an adaptive unscented Kalman filter. *J. Energy Storage* **2022**, *50*, 104553. [CrossRef]
61. Ma, L.; Hu, C.; Cheng, F. State of Charge and State of Energy Estimation for Lithium-Ion Batteries Based on a Long Short-Term Memory Neural Network. *J. Energy Storage* **2021**, *37*, 102440. [CrossRef]
62. Wang, Y.X.; Chen, Z.; Zhang, W. Lithium-ion battery state-of-charge estimation for small target sample sets using the improved GRU-based transfer learning. *Energy* **2022**, *244*, 123178. [CrossRef]
63. Chen, J.; Zhang, Y.; Li, W.; Cheng, W.; Zhu, Q. State of charge estimation for lithium-ion batteries using gated recurrent unit recurrent neural network and adaptive Kalman filter. *J. Energy Storage* **2022**, *55*, 105396. [CrossRef]
64. Cui, Z.; Kang, L.; Li, L.; Wang, L.; Wang, K. A combined state-of-charge estimation method for lithium-ion battery using an improved BGRU network and UKF. *Energy* **2022**, *259*, 124933. [CrossRef]
65. Jiao, M.; Wang, D.; Qiu, J. A GRU-RNN based momentum optimized algorithm for SOC estimation. *J. Power Source* **2020**, *459*, 228051. [CrossRef]

66. Chen, Z.; Zhao, H.; Zhang, Y.; Shen, S.; Shen, J.; Liu, Y. State of health estimation for lithium-ion batteries based on temperature prediction and gated recurrent unit neural network. *J. Power Source* **2022**, *521*, 230892. [CrossRef]
67. Fan, Y.; Xiao, F.; Li, C.; Yang, G.; Tang, X. A novel deep learning framework for state of health estimation of lithium-ion battery. *J. Energy Storage* **2020**, *32*, 40–42. [CrossRef]
68. Cui, S.; Joe, I. A Dynamic Spatial-Temporal Attention-Based GRU Model with Healthy Features for State-of-Health Estimation of Lithium-Ion Batteries. *IEEE Access* **2021**, *9*, 27374–27388. [CrossRef]
69. Fan, X.; Zhang, W.; Zhang, C.; Chen, A.; An, F. SOC estimation of Li-ion battery using convolutional neural network with U-Net architecture. *Energy* **2022**, *256*, 124612. [CrossRef]
70. Cui, Z.; Kang, L.; Li, L.; Wang, L.; Wang, K. A hybrid neural network model with improved input for state of charge estimation of lithium-ion battery at low temperatures. *Renew. Energy* **2022**, *198*, 1328–1340. [CrossRef]
71. Li, Y.; Li, K.; Liu, X.; Li, X.; Zhang, L.; Rente, B.; Sun, T.; Grattan, K.T.V. A hybrid machine learning framework for joint SOC and SOH estimation of lithium-ion batteries assisted with fiber sensor measurements. *Appl. Energy* **2022**, *325*, 119787. [CrossRef]
72. Gong, Q.; Wang, P.; Cheng, Z. A novel deep neural network model for estimating the state of charge of lithium-ion battery. *J. Energy Storage* **2022**, *54*, 105308. [CrossRef]
73. Li, P.; Zhang, Z.; Grosu, R.; Deng, Z.; Hou, J.; Rong, Y.; Wu, R. An end-to-end neural network framework for state-of-health estimation and remaining useful life prediction of electric vehicle lithium batteries. *Renew. Sustain. Energy Rev.* **2022**, *156*, 111843. [CrossRef]
74. Yang, N.; Song, Z.; Hofmann, H.; Sun, J. Robust State of Health estimation of lithium-ion batteries using convolutional neural network and random forest. *J. Energy Storage* **2022**, *48*, 103857. [CrossRef]
75. Li, Y.; Li, K.; Liu, X.; Wang, Y.; Zhang, L. Lithium-ion battery capacity estimation—A pruned convolutional neural network approach assisted with transfer learning. *Appl. Energy* **2021**, *285*, 116410. [CrossRef]
76. Zhou, D.; Li, Z.; Zhu, J.; Zhang, H.; Hou, L. State of Health Monitoring and Remaining Useful Life Prediction of Lithium-Ion Batteries Based on Temporal Convolutional Network. *IEEE Access* **2020**, *8*, 53307–53320. [CrossRef]
77. Fasahat, M.; Manthouri, M. State of charge estimation of lithium-ion batteries using hybrid autoencoder and Long Short Term Memory neural networks. *J. Power Source* **2020**, *469*, 228375. [CrossRef]
78. Chen, J.; Feng, X.; Jiang, L.; Zhu, Q. State of charge estimation of lithium-ion battery using denoising autoencoder and gated recurrent unit recurrent neural network. *Energy* **2021**, *227*, 120451. [CrossRef]
79. Wu, J.; Chen, J.; Feng, X.; Xiang, H.; Zhu, Q. State of health estimation of lithium-ion batteries using Autoencoders and Ensemble Learning. *J. Energy Storage* **2022**, *55*, 105708. [CrossRef]
80. Sun, Y.; Zhang, J.; Zhang, K.; Qi, H.; Zhang, C. Battery state of health estimation method based on sparse auto-encoder and backward propagation fading diversity among battery cells. *Int. J. Energy Res.* **2021**, *45*, 7651–7662. [CrossRef]
81. Son, S.; Jeong, S.; Kwak, E.; Kim, J.H.; Oh, K.Y. Integrated framework for SOH estimation of lithium-ion batteries using multiphysics features. *Energy* **2022**, *238*, 121712. [CrossRef]
82. Battery Data Center for Advanced Life Cycle Engineering, University of Maryland. Available online: https://calce.umd.edu/battery-data (accessed on 1 December 2022).
83. Yang, F.; Li, W.; Li, C.; Miao, Q. State-of-charge estimation of lithium-ion batteries based on gated recurrent neural network. *Energy* **2019**, *175*, 66–75. [CrossRef]
84. Zhang, R.; Xia, B.; Li, B.; Cao, L.; Lai, Y.; Zheng, W.; Wang, H.; Wang, W.; Zhang, R.; Xia, B.; et al. State of the Art of Lithium-Ion Battery SOC Estimation for Electrical Vehicles. *Energies* **2018**, *11*, 1820. [CrossRef]
85. Chaoui, H.; Ibe-Ekeocha, C.C.; Gualous, H. Aging prediction and state of charge estimation of a LiFePO4 battery using input time-delayed neural networks. *Electr. Power Syst. Res.* **2017**, *146*, 189–197. [CrossRef]
86. Han, X.; Lu, L.; Zheng, Y.; Feng, X.; Li, Z.; Li, J.; Ouyang, M. A review on the key issues of the lithium ion battery degradation among the whole life cycle. *eTransportation* **2019**, *1*, 100005. [CrossRef]
87. Lu, L.; Han, X.; Li, J.; Hua, J.; Ouyang, M. A review on the key issues for lithium-ion battery management in electric vehicles. *J. Power Source* **2013**, *226*, 272–288. [CrossRef]
88. Wang, D.; Miao, Q.; Pecht, M. Prognostics of lithium-ion batteries based on relevance vectors and a conditional three-parameter capacity degradation model. *J. Power Source* **2013**, *239*, 253–264. [CrossRef]
89. Diao, W.; Pecht, M.; Liu, T. Management of imbalances in parallel-connected lithium-ion battery packs. *J. Energy Storage* **2019**, *24*, 100781. [CrossRef]
90. Park, J.; Lee, J.; Kim, S.; Lee, I. Real-Time State of Charge Estimation for Each Cell of Lithium Battery Pack Using Neural Networks. *Appl. Sci.* **2020**, *10*, 8644. [CrossRef]
91. Gabbar, H.A.; Othman, A.M.; Abdussami, M.R. Review of Battery Management Systems (BMS) Development and Industrial Standards. *Technologies* **2021**, *9*, 28. [CrossRef]
92. Najafabadi, M.M.; Villanustre, F.; Khoshgoftaar, T.M.; Seliya, N.; Wald, R.; Muharemagic, E. Deep learning applications and challenges in big data analytics. *J. Big Data* **2015**, *21*, 1. [CrossRef]
93. Yang, F.; Zhang, S.; Li, W.; Miao, Q. State-of-charge estimation of lithium-ion batteries using LSTM and UKF. *Energy* **2020**, *201*, 117664. [CrossRef]
94. Chemali, E.; Kollmeyer, P.; Preindl, M.; Ahmed, R.; Emadi, A. Long Short-Term Memory-Networks for Accurate State of Charge Estimation of Li-ion Batteries. *IEEE Trans. Ind. Electron.* **2017**, *65*, 6730–6739. [CrossRef]

95. Song, X.; Yang, F.; Wang, D.; Tsui, K.L. Combined CNN-LSTM Network for State-of-Charge Estimation of Lithium-Ion Batteries. *IEEE Access* **2019**, *7*, 88894–88902. [CrossRef]
96. Hannan, M.A.; Lipu, M.S.H.; Hussain, A.; Ker, P.J.; Mahlia, T.M.I.; Mansor, M.; Ayob, A.; Saad, M.H.; Dong, Z.Y. Toward Enhanced State of Charge Estimation of Lithium-ion Batteries Using Optimized Machine Learning Techniques. *Sci. Rep.* **2020**, *10*, 4687. [CrossRef]
97. Hannan, M.A.; Lipu, M.S.H.; Hussain, A.; Saad, M.H.; Ayob, A. Neural network approach for estimating state of charge of lithium-ion battery using backtracking search algorithm. *IEEE Access* **2018**, *6*, 10069–10079. [CrossRef]
98. Lipu, M.S.H.; Hussain, A.; Saad, M.H.M.; Hannan, M.A. Optimal neural network approach for estimating state of energy of lithium-ion battery using heuristic optimization techniques. In Proceedings of the 2017 6th International Conference on Electrical Engineering and Informatics (ICEEI), Langkawi, Malaysia, 25–27 November 2017; pp. 1–6. [CrossRef]
99. Chai, X.; Gu, H.; Li, F.; Duan, H.; Hu, X.; Lin, K. Deep learning for irregularly and regularly missing data reconstruction. *Sci. Rep.* **2020**, *10*, 3302. [CrossRef]
100. Wang, L.; Wang, Y. A joint matrix minimization approach for seismic wavefield recovery. *Sci. Rep.* **2018**, *8*, 2188. [CrossRef]
101. Maddikunta, P.K.R.; Srivastava, G.; Gadekallu, T.R.; Deepa, N.; Boopathy, P. Predictive model for battery life in IoT networks. *IET Intell. Transp. Syst.* **2020**, *14*, 1388–1395. [CrossRef]